The role of ionic liquids in resolving the interfacial chemistry for (quasi-) solid-state batteries

Fanglin Wu [a,b,c], Zhen Chen [d], Shan Fang [e,**], Wenhua Zuo [f], Guk-Tae Kim [b,c,g], Stefano Passerini [b,c,h,*]

[a] State Key Laboratory of Advanced Technology for Materials Synthesis and Processing, Wuhan University of Technology, Wuhan 430070, China
[b] Helmholtz Institute Ulm (HIU), Helmholtzstrasse 11, Ulm 89081, Germany
[c] Karlsruhe Institute of Technology (KIT), P.O. Box 3640, Karlsruhe 76021, Germany
[d] Key Laboratory of Engineering Dielectric and Applications (Ministry of Education), School of Electrical and Electronic Engineering, Harbin University of Science and Technology, Harbin 150080, China
[e] School of Physics and Materials, Nanchang University, Nanchang, Jiangxi 330031, China
[f] Chemical Sciences and Engineering Division, Argonne National Laboratory, 9700 South Cass Avenue, Lemont, IL 60439 USA
[g] Department of Energy Convergence Engineering, Cheongju University, Cheongju, Chungbuk 28503, Republic of Korea
[h] Chemistry Department, Sapienza University of Rome, Piazzale a. Moro 5, Rome 00185, Italy

Keywords:
Solid state battery
Interface engineering
Ionic liquids
Solid electrolyte
Ion transport

A B S T R A C T

Interfacial issues impede the advancement of current solid state battery technology; thus, interface engineering approaches are necessary to enable solid-state configuration. The advantage of solid-state cells stems from their low flammability and high electrochemical stability. Ionic liquids are viscous and nonflammable compounds that possess the requisite physical properties while optimizing the interface between solid electrodes and solid electrolytes, accelerating interfacial ion transport and enabling the fabrication of engineered interphases via the supply of robust chemical building blocks. This review summarizes the roles of ionic liquids in solid-state batteries focusing on the interface, with insights into their functionality as well as highlighting their applicability in the next generation battery systems.

1. Introduction

Carbon neutrality has been pledged by more than 140 countries during the latest COP26 conference [1,2], propelling rechargeable batteries to the centre stage of energy storage and conversion technology to enable electrification of transport and mobile applications. Nonetheless, the state-of-the-art lithium-ion batteries fail to satisfy the ever-increasing demands of electric vehicles that require a specific energy of up to 500 Wh kg ^{1} [3,4]. Various battery systems are energetically exploited to boost the energy density enabling prospective next generation battery technologies, among these, solid state batteries (SSBs) are regarded as the successor that will seize the markets of electric vehicles [5]. SSBs are generally classified into all-solid-state batteries (ASSBs) and quasi-solid-state batteries (QSSBs), with these latter involving the presence of small liquid electrolyte amounts [6,7]. These latter offer enhanced electrode/electrolyte interfaces and, somehow surprisingly, reduced metal dendrite growth, only slightly compromised thermal stability if proper liquid electrolyte are selected [8], and simplified mass production [9]. The main advantage of SSBs is their superior safety property enabled by the core component, the solid electrolyte (SE) which exhibits high thermal stability as well as nonflammability [10], although it is doubted this latter claim is not fully confirmed for commercial cells [11]. Another significant advantage lies in the substitution of conventional graphite anode with lithium metal. The latter is endowed with high specific capacity and low (electrochemical) potential, which was predicted to achieve an increased volumetric and gravimetric energy density by ~70 % and 40 %, respectively [10]. Additionally, a wider electrochemical stability window (ESW) of SE allows the cells to operate at a higher voltage, up to 5 V when combined with high voltage cathodes such as lithium-rich layered oxides[12] or $LiNi_{0.5}Mn_{1.5}O_4$ [13], further elevating the energy and power density of the cells. Under such circumstances, SSBs composed of

* Corresponding author at: Helmholtz Institute Ulm (HIU), Helmholtzstrasse 11, Ulm 89081, Germany.
** Corresponding author.
E-mail addresses: fangshan@ncu.edu.cn (S. Fang), stefano.passerini@kit.edu (S. Passerini).

a high-energy cathode, stable SE, and metallic anode is regarded as a promising configuration.

With the continual development of SE, a variety of SEs have been explored to achieve comparable or even higher ionic conductivity with respect to that of the conventional organic electrolyte, especially sulfide-based superionic conductors such as $Li_{9.54}Si_{1.74}P_{1.44}S_{11.7}Cl_{0.3}$ (25 mS cm ^{1}) [14]. Therefore, the remaining challenge of SE has shifted from the previous (crucial) issue of low ionic conductivity to interfacial issues, as the interfacial chemistry gradually becomes the bottleneck for SSBs [15,16]. The interfacial issues mainly originate from the immobility of SEs which limits the electrolyte flowing or infiltrating into gaps or voids in SSBs [17], resulting in generally poor physical contact between electrodes (cathode or anode) and electrolyte, and between particles within the cathode electrode as well as the SE [18]. Besides, other issues are present on the cathode side, such as the space-charge layer [19,20], chemical reaction between cathode and SE [21–23], large volumetric change of cathodes during charge/discharge [24–26]. Whereas, on the anode side, issues such as interfacial compatibility against lithium metal anode (LMA) [16] or sodium metal anode (SMA) [27] and the growth of lithium (sodium) dendrites [28,29] must be resolved. Various strategies were adopted to tackle these interfacial issues between SEs and electrodes, such as atomic layer deposition (ALD) technology [30–32], *in-situ* solidification technology [33], three-dimensional construction of interlayer [34,35]. These approaches effectively mitigate such shortcomings to a certain extent, nevertheless, without regard to technical difficulty or cost. Recently, the vital role of ionic liquids (ILs) on the interface of SSBs cannot be neglected, considering their similarities to SEs, notably nonflammability and high thermal stability. Additionally, ILs exhibit excellent compatibility with lithium (as well as sodium) metal and high fluidity enabling ILs as an ideal mediator to solve the interface issues of SSBs [36,37]. Since 2010, the number of publications dealing with the introduction of ILs into SSBs has gradually increased (Fig. 1), indicating the potentiality of ILs in the field of SSBs.

In this review, the focus is on the latest advances in IL modified SSBs based on the functions of ILs. The different roles of ILs are comprehensively discussed, especially the capabilities of ILs in modifying the interfacial contact of inorganic solid electrolytes (ISE). The unique electrochemistry of ILs and their underlying mechanism which can enhance the performance of SSBs is also elucidated. Finally, the challenges and future prospects of applying ILs in (quasi-) solid state batteries are outlined.

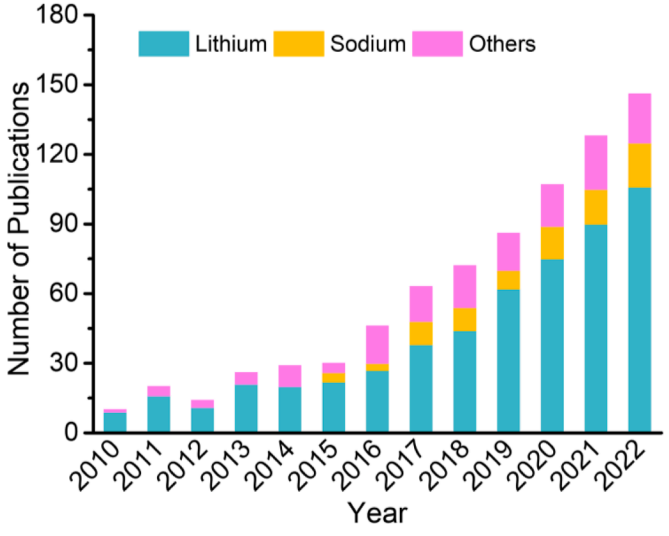

Fig. 1. The number of publications of ILs-employed in SSBs since 2010 (Data retrieved from "Web of Science").

2. The advantages and properties of ILs

ILs are molten salts with low temperature melting points (below 100 °C) [38,39], composed of a large framework cation and a charge-delocalized anion, with weak ion interaction, fast ion migration, and thus a relatively high ionic conductivity [40]. First, owing to the electrostatic interaction, ILs are poorly volatility, and in some cases poorly flammable [37,41]. Most ILs possess much superior thermal stability comparing with carbonate-based electrolytes, generally showing no pyrolysis below 300 °C [42], which is advantageous for application in SSBs without sacrificing the overall safety. As regard to the ILs work with the highly charged electrodes [43]. Yamaki et al. [44] observed the exothermic peaks started from around 190 °C in the coexistence of carbonate-based electrolytes and charged $Li_{0.46}CoO_2$, however, no peak was detected below 260 °C in $Li_{0.46}CoO_2$ in contact with mixed electrolytes composed of carbonate electrolytes and ILs (EMITFSI + CEMATFSI). This clearly demonstrates that ILs are less reactive toward oxygen release and, more in general, aggressive delithiated electrodes. Sakaebe et al. [45] reported no exothermic reaction occurring below 300 °C for the 0.32m LiTFSI in PP_{13}TFSI IL in contact with charged $Li_{1-x}CoO_2$ employing differential scanning calorimetry (DSC) analysis. Nevertheless, the thermal stability of ILs depend on their cations or anions, e.g. EMI^+ type ILs own an inferior safety than $BMIM^+$, Py_{13}^+, Pp_{14}^+ and $TMBA^+$, as well as FSI offers poorer thermal stability than TFSI [46].

Second, some ILs show excellent compatibility against the lithium metal anode (LMA), yielding to another great advantage of ILEs. Conventional carbonate-based liquid electrolytes do not prevent lithium dendrites growth resulting in the short circuit of cells [47,48]. On the other hand, ILEs were demonstrated yielding highly stable lithium metal batteries without evidence of dendrite growth or thermal runaway, benefitting of the robust SEIs consisting of inorganic species (LiF, Li_2CO_3, $LiSO_2F$, LiOH) and cation-breakdown products [49]. The long aliphatic chain of IL is beneficial to suppress the dendrites growth by virtue of the combined effects of electrostatic shielding and lithiophobicity, while the anion is involved into the formation of a LiF-predominant SEI layer [50]. Third, ILs generally own a wide electrochemical stability, in some cases even reach 6 V, their wide ESWs is ideal for their application in high voltage SSBs. Last, the unlimited structural variations of the constituent ions allow the design of ILs with specific properties.

The cations of commonly applied ILs are mainly pyrrolidinium (N-methyl-N-propylpyrrolidinium, N-butyl-N-methylpyrrolidinium), piperidinium, imidazolium, and quaternary ammonium, while the anions focus on the commonly utilized bis(fluorosulfonyl)imide (FSI), bis (trifluoromethanesulfonyl) imide (TFSI) and tetrafluoroborate (BF_4). Some properties of typical ILs are compared in Table 1. The pioneer investigation of imidazolium-based ILs dates back to the 1990s [51], afterwards, significant attention focused on their use in lithium batteries due to their advantages of high ionic conductivity and low viscosity. For example, the IL composed of 1-ethyl-3-methyl imidazolium cation ($EMIM^+$) and FSI anion was reported with a superior ionic conductivity of 7.71×10^{3} S cm ^{1}, approaching the level of commercial organic electrolytes [52] However, the three acidic protons on the unsaturated five-membered ring tend to cause cation reduction [53], resulting in poor compatibility against lithium metal or carbon and hindering the application of imidazolium-based ILs in lithium batteries. In contrast, quaternary ammonium-based ILs generally possess excellent electrochemical stability, verified by the higher oxidation potential >5.0 V vs. Li/Li^+ and a reduction potential lower than 0 V vs. Li/Li^+ [42]. However, high stability generally comes with a high viscosity, the latter leads to poor wettability with electrodes unless an elevated temperature is applied. Piperidinium-based ILs belong to a quaternary ammonium structure but with a six-membered ring, which exhibits superior electrochemical stability (attaining 5.7 V vs. Li/Li^+) than that of the traditional quaternary ammonium-based ILs. Unfortunately, the ionic

Table 1
Comparison of the properties of common ILs (or ILEs).

Ionic Liquids	Viscosity (cp)	Ionic conductivity (S cm ^{1})	ESW (vs. Li/Li^{+})	Thermal stability (TGA analysis)
Imidazolium based IL [56,57]	25–45 (20 °C)	>1 × 10 ^{3}	≤ 5 V	>300 °C
Quaternary ammonium based IL [56,58]	>80 (20 °C)	1.0 × 10 ^{5} ~4.7 × 10 ^{4}	≥ 5 V	>350 °C
Asymmetrical Imidazolium trialkylammonium dicationic IL [59]	>50	5.0 × 10 ^{5} ~2.7 × 10 ^{4}	4~5 V	
Pyrrolidinium based ILE (Pry14FSI+LiTFSI) [60]	17-396 (mPa/s) (80-0 °C)	~2.5 × 10 ^{3} (25 °C)	~5 V	
Pyrrolidinium based ILE (Pyr13FSI+LiTFSI) [61]	40~76 (25 °C)	4.8 × 10 ^{3} ~9.9 × 10 ^{3} (25 °C)		
Pyrrolidinium based ILE (C4mpyr-TFSI+LiTFSI+$LiNO_3$) [62]	47.5 (23 °C)	2.7 × 10 ^{3} (23 °C)		
Pyrrolidinium based ILE (Pyr14TFSAM+LiTFSAM+VC) [63]		3.8 × 10 ^{3}~12.6 × 10 ^{3} (20~60 °C)	~4.5 V	Decomposition from 283 °C
Piperidinium based ILE ([MMEPip][TFSI]+LiTFSI-EC-DEC) [64]	33–403 (mPa/s) (65~25 °C)	1.35 × 10 ^{3}~6.8 × 10 ^{2} (5~30 °C)	~5 V	Decomposition from 300 °C
Piperidinium based ILE (PipGuan-TFSI+LiTFSI) [65]	164 (25 °C)	0.74 × 10 ^{3} (20 °C)	4.4 V	Decomposition from 415 °C
Piperidinium based ILE (C_6O_2(mpip)$_2TFSI_2$+LiTFSI) [66]		0.39 × 10 ^{3} (60 °C)	6 V	Decomposition from 360 °C
Piperidinium based ILE (C_{1O1}mpip][FSI]+LiFSI) [67]	56 (30 °C)	5 × 10 ^{3} (30 °C)	4.7V (Pure IL)	Decomposition from 238 °C
Piperidinium based ILE (C_{1O1}mpip][TFSI]+LiTFSI) [67]	108 (30 °C)		5.2V (Pure IL)	Decomposition from 282 °C

conductivity is only ~1.5 mS cm ^{1} at room temperature due to higher viscosity [42,54,55].

Considering the diverse properties, only a small proportion of ILs satisfy the demands for application in SSBs, for instance, appropriate ionic conductivity and high voltage resistance. The ILs applied to (quasi-) SSB systems should be designed with a focus on balancing the relationships between ionic conductivity, viscosity and ESW. For example, the five-membered-ring pyrrolidinium-based ILs are suitable candidates that have been widely investigated as nonflammable and high safety electrolytes for Li-metal batteries [60,68,69], since they achieve a good balance between ionic conductivity (> 10 ^{3} S cm ^{1}) and electrochemical stability (ESW of > 5.0 V), as well as an excellent compatibility with lithium metal.

3. The roles of ILs in (quasi-) SSBs

ILs were firstly introduced into "polymer-and-salt" SEs since 1995 [70]. After, Li-ion conductive solid polymer electrolytes (SPE) were investigated and developed [71–73]. In 2010, polymeric ionic liquid was prepared and employed into Li/$LiFePO_4$ solid-state cells and obtained an outstanding performance [74], soon, a novel quasi-solid-state composite electrolyte was firstly designed in a Li/$LiFePO_4$ cell [75]. In the meantime, the $LiZnSO_4F$ SE functionalized with IL interlayer were reported with a dramatically improved ionic conductivity [76]. Since that, ILs attracted increasing attention for application in SSBs, especially focused on the SEs interface. The development route of ILs in SSBs are displayed in Fig. 2.

Generally, ILs play four roles in SSBs, acting as interfacial wetting agents (including cathode and anode side), poly(ionic liquids) (PILs) electrolytes, hybrid electrolytes, and plasticizers for other polymer-type electrolytes (Fig.3), which are discussed in the following sections.

3.1. ILs as wetting agent for SE/electrode interface

Although the ionic conductivity of SEs has been greatly improved, the interfaces between SEs and electrodes are still the rate-determining step for ion migration. On account of the rigidity of SEs, the restricted and uneven solid-solid contact confines the ion transport across the interface and induces hot spots for the formation of lithium dendrites [77,78]. More importantly, the sulfide/oxide-based electrolytes react with LMA due to their high reactivity causing severe degradation at the interface [10]. Recently, a simple and effective liquid phase therapy method was employed to modify the solid-solid interface, utilizing a small amount of liquid (<10 μL cm ^{2}, not included that in the composite cathode). The consequent chemical/electrochemical reactions occurring at the interface improve the ion transport across the multiple interfaces in SSBs, resulting in enhanced interfacial stability, as shown in Fig. 4, while some key performances are summarized in Table 2. Additionally, the liquid can also fill the voids at the interface to enhance the contact between electrodes/SEs [79]. Carbonate-based electrolyte were discovered to *in situ* form a beneficial solid electrolyte interphase (SEI) layer with oxide-based SEs [80], ameliorating the rate performance. Afterwards, small amounts of organic electrolytes were applied as an agent to wet the interface of electrodes/SEs [34,81,82]. Nevertheless, the introduction of carbonate electrolyte inevitably compromises the main advantage of SEs, the safety. In contrast, this drawback can be

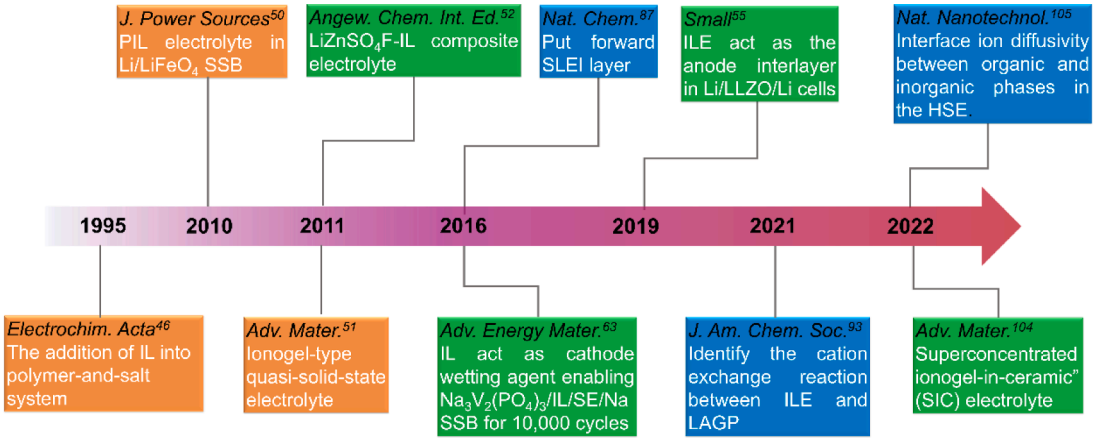

Fig. 2. Development of ILs in SSB system.

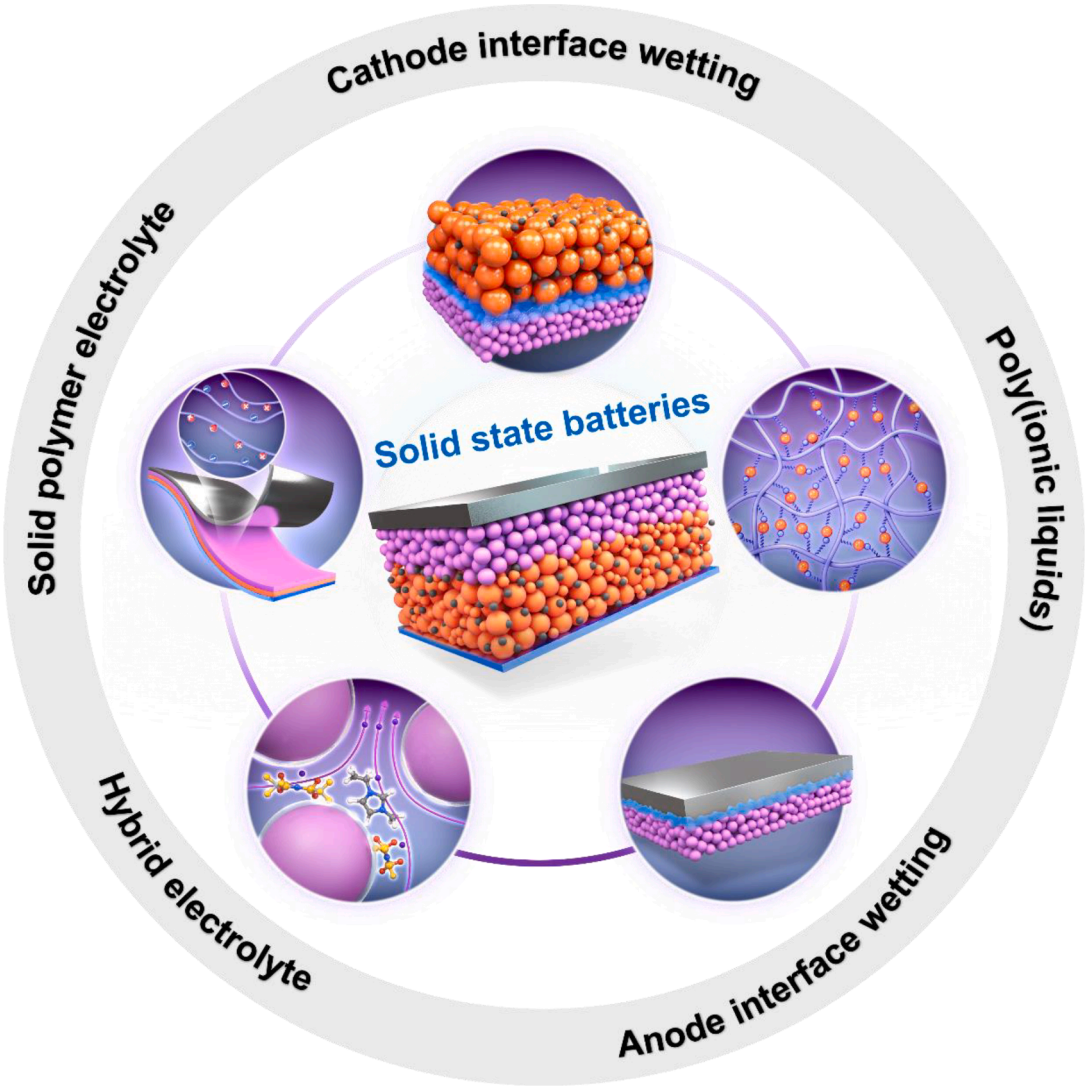

Fig. 3. Schematic illustration of the various roles of ILs in SSBs.

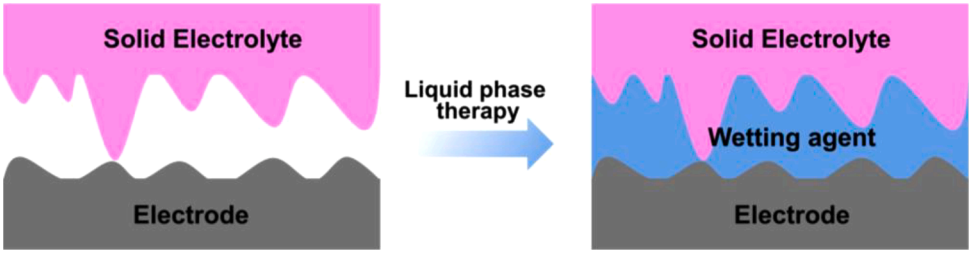

Fig. 4. Schematic diagrams of liquid phase therapy in solid state lithium metal batteries. Reproduced with permission [78]. Copyright 2020, Elsevier.

avoided by replacing carbonate-based electrolyte with ILs as the interface wetter, which could resolve the interface issues and maintain the excellent nonflammability. Herein, the role of ILs as interfacial wetting agent at cathodes/SE and anodes/SE interface is discussed.

3.1.1. The interface between cathode and SE

Due to the absence of liquid fluidity, the cell faces a large interfacial resistance due to the loose contact between cathode and ISE, resulting in sluggish charge-transfer at the interface, limiting the cell performance especially at a high current. In addition, the poor electronic and ionic conductivity at the interparticle interface as well as the shrinkage and expansion of cathode particles during charge/discharge processes exacerbate the contact loss [92]. A suitable liquid additive acting as the interfacial wetting agent to improve the interfacial contact is fundamental. The ideal wetting agent should satisfy the following requirements: (1) satisfactory ionic conductivity, (2) high voltage resistance, (3) good wettability, (4) nonflammability. Considering these factors, ILs are suitable candidates as interfacial wetting agent to modify the cathodes/SEs interface.

3.1.1.1. Coating IL onto cathodes. In 2012, Sagane et al. [93] investigated the interface between lanthanum lithium titanate ISE and

Table 2
Comparison of the performance of ILs as interfacial wetting agent.

Functions of ILs	Types of ILs	Usage of ILs	Solid electrolyte	Cathode/Anode	Performance	Refs.
Cathode interface wetting	$PP_{13}FSI$	5 μL cm^{-2}	$Na_{3.3}Zr_{1.7}La_{0.3}Si_2PO_{12}$	NVP/Na	10000 cycles without decay at 10C and RT	[83]
Cathode interface wetting	$PP_{13}TFSI$	1 μL cm^{-2}	LLZTO	LCO@LLZNO/Li	80.2 % after 400 cycles at 0.2C and 60 °C	[84]
Cathode interface wetting	$PP_{13}BF_4$	2 wt.%	PEO-based SSE	LCO/Li	76.3 % after 100 cycles at 0.2C and 55 °C	[85]
Cathode interface wetting	$LiClO_4$/BMIMTFSI	1.13 μL cm^{-2}	LLZTO	NCM622/Li	87.6 % after 100 cycles at 0.2C and 60 °C	[86]
Composite cathode	LiTFSI/EMITFSI	11 wt.%	Al-doped LLZO	LCO/Li	80 % after 100 cycles at 60 °C	[87]
Composite cathode	LiTFSI/ $Pyr_{14}TFSI$	18.8 wt.%	LLZTO-MCL	LCO/LI	81.1 % after 300 cycles at 0.2C and RT	[88]
Composite cathode	$Pyr_{14}FSI$	40 wt.%	Na-β″-Al_2O_3	$Na_{0.66}Ni_{0.33}Mn_{0.67}O_2$	90 % after 10000 cycles at 6C and 70 °C	[89]
Anode interface wetting	LiTFSI-$Pyr_{14}FSI$	2.65 μL cm^{-2}	LLZO	LFP/Li	45 cycles without decay at 20 mA g^{-1} and 25 °C	[79]
Anode interface wetting	LiTFSI-$Pyr_{13}TFSI$	~10 μL	LGPS	S@C/Li	82.6 % after 50 cycles at 83.5 mA g^{-1} and RT	[90]
Anode interface wetting	NaTFSI/$Pyr_{14}TFSI$	≤5 μL	Na_3SbS_4	FeS_2/Na	~62 % after 330 cycles at 100 mA g^{-1} and RT	[91]

different ILs based on AC impedance method. It was uncovered that the activation energy was influenced by the anion species of ILs, rather than the cations. Currently, the anion of ILs applied as interfacial wetting agents are mainly FSI or TFSI anions coupled with the propylpiperidinium-based or pyrrolidinium-based cations. These IL groups have demonstrated an outstanding electrochemical stability at high voltage which benefits the formation of a robust cathode electrolyte interphase (CEI) layer [69,94,95]. Therefore, they have been chosen as wetting agent and demonstrated significant improvement of the cell performance. For example, a small amount of nonflammable, N-methyl-N-propylpiperidinium-bis(fluorosulfonyl) imide ($PP_{13}FSI$) was used as a wetting agent to construct $Na_3V_2(PO_4)_3$/IL/SE/Na cells, obtaining an exceptional cycling stability via maintaining a capacity of ~90 mAh g^{-1} without decay after 10,000 cycles at 10 C (Fig. 5a) [83]. In contrast, the $Na_3V_2(PO_4)_3$/SE/Na cells without IL exhibit a low discharge capacity of 85 mAh g^{-1} and with a severe capacity degradation to 44 mAh g^{-1} after only 10 cycles. To further certify the superiority of IL for interfacial engineering, an equivalent amount of organic carbonate electrolyte (0.8M $NaPF_6$ in EC/DMC) was employed which resulted in a sharp capacity degradation after 250 cycles at 0.2 C. The introduction of IL not only effectively enhanced the interfacial contact but also provided a new ion transport channel, facilitating ion migration between active materials particles and SE particles. Additionally, the IL could create a beneficial buffer space to offset the volume expansion for the cathode materials upon cycling (Fig. 5b, c) [83]. Bi et al. [84] focused on the interface engineering at cathode side partially coating $Li_{6.375}La_3Zr_{1.375}Nb_{0.625}O_{12}$ (LLZNO) on the $LiCoO_2$ and combining an intermediate layer of N-methyl-N-propylpiperidinium bis(trifluoromethanesulfonyl)imide ($PP_{13}TFSI$) (Fig. 5d); this achieved a capacity retention of above 80 % after 400 cycles at 0.2 C and 60 °C. The IL formed good contact between cathode and SE, moreover, the decomposition of IL generated an ionic conducting CEI layer which is beneficial to promote lithium-ion transport.

3.1.1.2. Mixing ILs and active materials for composite cathode. Besides dropping a little amount of IL on the cathode surface, adding IL into the cathode slurry during the preparation of positive electrode is also a viable route. The introduction of small IL amount would not alter the current electrode fabrication engineering apart from slightly effect in the rheological behavior of the resuting slurries. Cheng et al. [87] designed an EMI-based IL-containing $LiCoO_2$ composite cathode, the interfacial resistance of SE/electrode was significantly reduced from 500,000 to ~100 Ω cm^2. However, the QSSB endured an evident performance decay, maintaining a capacity retention of ~80 % after 100 cycles at 60 °C, which was deemed to be caused by the thermal or electrochemical instability of the IL. Sun's group[88] prepared a composite cathode by introducing a more electrochemical stable IL, N-butyl-N-methylpyrrolidinium bis(trifluoromethanesulfonyl)imide ($Pyr_{14}TFSI$), as the wetting agent. The developed full cell obtained a high capacity retention of 81.1 % after 300 cycles at 0.2 C and room temperature. Liu et al. [89] designed a toothpaste-like electrode using $Pyr_{14}FSI$ mixing with sodium layered oxide $Na_{0.66}Ni_{0.33}Mn_{0.67}O_2$,

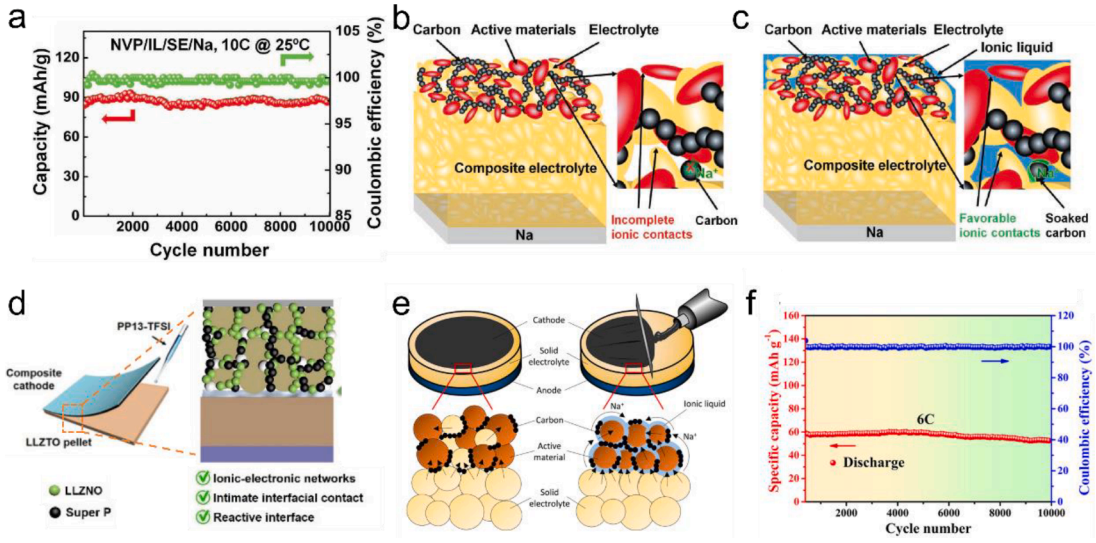

Fig. 5. Cycling performance of the (a) NVP/IL/SE/Na solid-state battery at 25 °C with a current rate of 10 C and (b) Schematic representation of the NVP/SE/Na and (c) NVP/IL/SE/Na solid-state batteries. Reproduced with permission [83]. Copyright 2017, Wiley. (d) Constructing island-like LLZNO coated cathode, and adding $PP_{13}TFSI$ at cathode-electrolyte interface. Reproduced with permission [84]. Copyright 2020, Elsevier. (e) Schematic diagrams of a conventional sintering type and the newly designed solid-state battery based on an inorganic ceramic electrolyte. (f) Long-term cycling performance. Specific capacity and Coulombic efficiency versus cycle number at 6 C rate. Reproduced with permission [89]. Copyright 2016, American Chemical Society.

combined with Na-β''-Al_2O_3 as SE (Fig. 5e), achieving an exceptional cycling reversibility with a capacity retention of 90 % after 10,000 cycles at 6 C and 70 °C (Fig. 5f). Furthermore, IL was applied to act as a bridge to connect bulk-sized garnet electrolyte and $LiFePO_4$ [96] or $LiMn_2O_4$[97] cathode, to reduce the electrode/SE interfacial resistance. Actually, FSI- and TFSI-based ILs can also lead to the *in-situ* formation of high ionically conducting inorganic species, such as LiF and Li_3N, at the cathode/SE interface resulting from the decomposition of the IL's anion, which further reduce the lithium ion transport to the interface [86]. It is worth mentioning that the presence of (liquid) ILs in the composite electrode may raise concerns about the effect of the stacking pressure. However, there is a lack of research work on this issue, which is worth a deep investigation in the near future.

In summary, ILs working as the interfacial wetter agent can be divided into two approaches: the dropping method, whereby a small amount (< 2 μL cm ^{2}) of IL is added onto the surface of positive electrode, to wet the poor interfacial contact between electrode and SE and fill the cathode porosity. This also contributes to the formation of a stable CEI layer for ion migration. The other method is mixing IL and cathode material to prepare a composite cathode, the IL and its corresponding decomposition products work as a bridge to connect SE particles and active materials, reducing the interparticle resistance in the electrode and between the electrode and SE.

3.1.2. *Metal anode/SE interface*

Comparing with the crucial and highly effective function of IL in boosting the electrochemical performance of the cathode/SE interface, the role of IL at the anode varies depending on the SE type. For instance, some polymer-based electrolytes have good compatibility against the metal anode and excellent flexibility, not needing the assistance of ILs in most cases [98,99]. However, inorganic-based electrolytes have poor contact with metal anode, the pore formation and surface contamination at the electrode/SE interface result in a large interfacial resistance especially for oxide-based SEs [100]. Although the pores can be reduced to a great extent by high stack pressures ($\geq$ 35 MPa) because of the plastic deformation of metal anode [100]. Additionally, a severe reduction reaction would occur in the case of NASICON-type SEs once in direct contact with metal anode, generating a ionic and electronic conducting mixed interphase, which can damage the solid pellets due to continuous parasitic reduction reactions along with a large volume expansion [101,102]. Adding a small amount of IL is an ideal solution considering that several ILs exhibit high compatibility with Li metal through the formation of a robust inorganic-based SEI protecting layer on the metal surface [103–105]. In contrast, the introduction of synthetic protecting layers, such as metal oxide coating layers [30,32], a polymer interlayer [34,106], or any high lithium ion and electron conductivities interlayer[107–109] would incur extra expenses due to the additional technology complexity. Yang's group[110] achieved a stable SEI layer in Li/$Li_{10}SnP_2S_{12}$/Li symmetric cells through the addition of a small amount of Pyr_{13}TFSI IL combined with 1.5 M LiTFSI salt. Apart from the IL acting as a wetting agent, a LiF-rich SEI layer was also formed to isolate the $Li_{10}SnP_2S_{12}$ electrolyte from LMA which demonstrated a steady lithium stripping/platting test for more than 1000 h (Fig. 6a). After, the lithium salt concentration in ionic liquid electrolyte (ILE) was decreased to 1 M, obtaining a remarkable interface stability with the interfacial resistance sharply dropping from 2021 to 142 Ω cm^2 (Fig. 6b) 90]. Additionally, the IL-modified LGPS enabled a high discharge capacity of 1017 mAh g ^{1} in lithium-sulfur SSB with a good capacity retention, attributed to an improved anodic interface contact (Fig. 6c). A similar result was also observed in sodium metal batteries in which a low concentration electrolyte of Pyr_{14}TFSI combined with NaTFSI was employed in Na/IL/Na_3SbS_4/IL/Na cell system. The stable SEI layer containing NaF and CF_3 components was detected, contributing to the generation of a stabilized interface between SE and SMA on

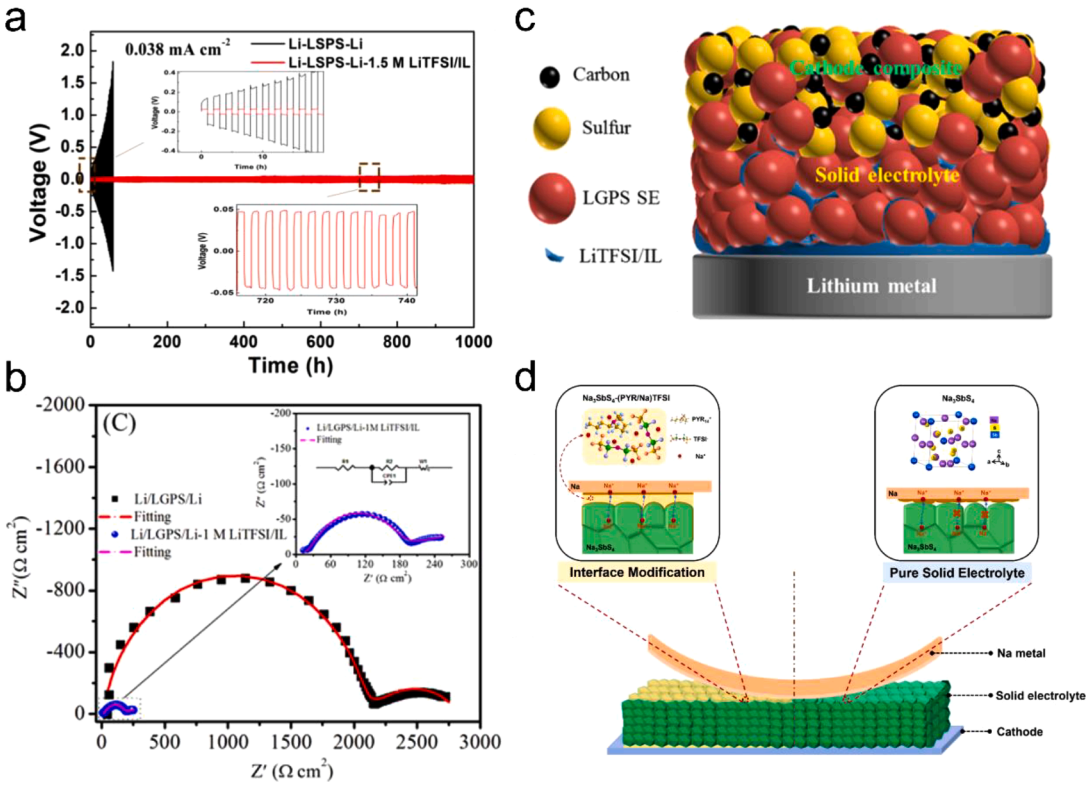

Fig. 6. (a) Li^+ stripping/plating curves of Li/LSPS/Li symmetric cells with and without 1.5 M LiTFSI/IL. Reproduced with permission [110]. Copyright 2018, American Chemical Society. (b) Nyquist profiles for the Li/LGPS/Li symmetric cells with and without 1 M LiTFSI/PYR_{13}TFSI IL. (c) Schematic diagram of the quasi-solid-state lithium-sulfur battery. Reproduced with permission [90]. Copyright 2019, American Chemical Society. (d) Schematic diagram of the Na_3SbS_4/Na interface with (PYR/Na)TFSI interlayer. Reproduced with permission [91]. Copyright 2022, Elsevier.

account of the suppressed adverse side reactions and the growth of sodium dendrites (Fig. 6d) [91]. However, in NASICON-type SEs, the formed SEI layer by adding ILs could not suppress the reduction reaction between SEs and metal anodes due to the thermal dynamic instability against metal anode. Albeit the improved cycling stability compared to the IL-free system, the introduction of IL could only protect the interface for a short time. The reduction reaction results in continually increasing interfacial resistance and final pulverization of SE pellets [111]. Hence, ILs were combined with a thin polymer protection layer (e.g. poly[2, 3-bis(2,2,6,6-tetramethylpiperidine-*N*-oxycarbonyl)norbornene] (PTNB) [112,113], or IL-based SPE [111]) to achieve enhanced interfacial stability. In summary, ILs appears to be very appropriate for sulfide-based or garnet-based ISEs as the anode wetting agent.

3.1.3. *The interface between IL and SE*

Once liquid electrolytes are added into the interface between SE and anode, not only a SEI layer but also a solid-liquid electrolyte interphase (SLEI) is generated [114], as shown in Fig. 7a. The SLEI layer is mainly comprised of inorganic compounds including the decomposition products of conducting salts and presumably solid electrolytes. The additional SLEI layer formed by conventional liquid electrolyte was predicted to decrease the gravimetric energy density by ~18 % in hybrid Li/S_8 cell (Fig. 7b), so a stable SLEI layer is equally important for the cell performance. The Janek group [100] investigated the working mechanism of IL interlayer between lithium metal and $Li_{6.25}Al_{0.25}La_3Zr_2O_{12}$ (LLZO) at a pressure less condition. They added one drop of $Pyr_{14}TFSI$ with LiTFSI salt on one side of the polished LLZO pellet and observed two additional semicircles (Fig. 7c–e), which can be assigned to the SLEI and SEI layers, respectively. In addition, they found the SEI at the Li/ILE interface is fairly stable while the SLEI at the ILE/LLZO interface grew with time and contributed the most resistance in the mid frequency region. Finally, they discovered that lower lithium salts concentration would benefit the cell performances, due to the likelihood of a lower viscosity of ILE resulting in a reduced surface tension. As a result, this produces superior "contact buffer" that can easily adapt to changes in the interface morphology by spreading to fill the generated voids.

3.2. *Inorganic-IL based hybrid electrolytes*

The IL additives discussed thus far function as wetting agent and the SEs are mainly pellet-type with a large thickness, which is impractical for industrial implementation; the thickness and flexibility should be further optimized. Therefore, one type of hybrid electrolytes (HEs) combining the excellent mechanical properties of ISEs and high fluidity of liquid electrolytes emerges [115,116]. ILs are proposed as solvents to mix with ISEs for the preparation of HEs, however, the most crucial

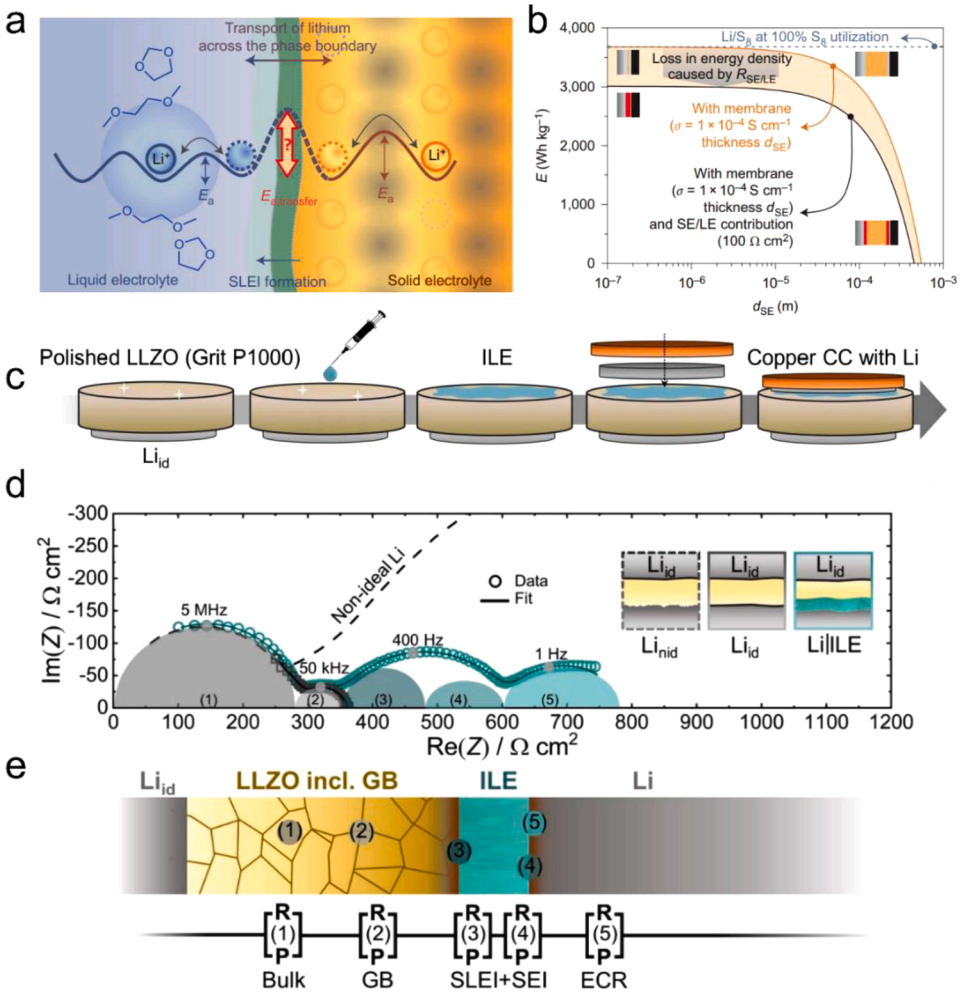

Fig. 7. (a) Schematics of ion transport and resistance contributions in cells with solid–liquid phase boundaries. (b) Loss in energy density of a hybrid Li/S_8 cell caused by the overpotentials that result from the solid-electrolyte membrane (ηSE) and the SE/LE interface (ηSE/LE) at a cycling rate of 1 C in correlation with the membrane thickness, dSE. Reproduced with permission [114]. Copyright 2016, Nature. (c) Schematic of the cell assembly process. (d) Comparison of Nyquist plots of impedances of $Li_{nid}|LLZO|Li_{id}$ (dashed), $Li_{id}|LLZO|Li_{id}$ (grey) and $Li|ILE|LLZO|Li_{id}$ (green) cells. (e) Schematic diagram of the investigated $Li|ILE|LLZO|Li_{id}$ cell alongside the used equivalent circuit for fitting and the corresponding origins in the cell. Reproduced with permission [100]. Copyright 2021, Wiley.

challenge for HEs remains the interfacial issues between IL and inorganic components. In this section, the latest developments of IL-containing HEs are summarized with focus on the interfacial issues between SEs and ILs (Table 3).

In 2011, Tarascon's group[76] reported a novel $LiZnSO_4F$ fluorosulfate phase via an IL-assisted synthesis route, and discovered that the functionalized $LiZnSO_4F$-IL composite ($LiZnSO_4F$ grains surrounded by Li-containing IL layer) could significantly enhance the ionic conductivity of Li-based conductors (Fig. 8a), although the corresponding precise nature of the interface effects remain unclear. Nevertheless, Appetecchi et al. [124] revealed that the simple mixing (coating) of NACISON-type SE ($Na_3Si_2Y_{0.16}Zr_{1.84}PO_{12}$) with $Pyr_{14}TFSI$ IL without sintering thermal treatment could not induce any synergic effect on the formed HE. It was suggested that a proper functionalization of the NASICON surface and/or IL is needed to promote the transport of sodium ions at the SE/IL interface. Interestingly, a thin pellet-type HE was prepared with a specific composition of 80 wt.% of LLZO, 19 wt.% of $Pyr_{14}TFSI$ and 1 wt.% of LiTFSI [118]. This HE gained an ionic conductivity of 0.4×10^{-3} S cm^{-1} as well as a wide ESW up to 5.5 V (Fig. 8b), and contributed to a high cycling stability with a capacity retention of 99 % after 150 cycles in full cells. The homogenous distribution of IL on the surface of ceramic particles probed by field emission scanning electron microscopy contributed to the superior electrochemical performances (Fig. 8c) [118]. Subsequently, a different cation-based IL of 1-butyl-1-methylpyrrolidinium bis(trifluoromethanesulfonyl) imide (BMPTFSI) was employed as a "soft" coating layer of $Li_7La_3Zr_2O_{12}$ to form a conducting network which greatly facilitated the lithium migration between SE/IL interface via transforming the ion conduction from a point-to-point pathway to a face-to-face pathway [81]. Hu et al. [119] reported a low-temperature IL method to prepare a nanosized Li-rich fluoride SE (Li_3GaF_6). The IL was solidified into nano-floccule which could serve as an *in-situ* binder to bond the adjacent nanoparticles (Fig. 8d, e), hence, achieved a high ionic conductivity of 10^{-4} S cm^{-1} at room temperature among fluoride SEs due to the improved lithium ion transport at the SE particles interfaces. Recently, the chemical reactions occurring at the interface between ISE and IL was investigated;[125]. $Li_{1.5}Al_{0.5}Ge_{1.5}(PO_4)_3$ (LAGP) and $Pyr_{13}TFSI$ were selected. A homogenous composition of LAGP-IL mixtures without a gradient of the elements was evidenced. The introduction of IL at a ratio of 5–10 % is capable of improving the ionic conductivity of LAGP via formation of an ionic bridge (Fig. 8f). In addition, at a low current condition, the diffusion of lithium ions was through both IL and LAGP. Nevertheless, the lithium ions transport was mainly observed within LAGP under a high current. These discoveries are beneficial to inform on the design of IL-based HEs.

Composite solid electrolytes (CSE) are SEs including inorganic solid ionic conductors and polymer(s) matrix, capable of offering the outstanding mechanical properties of ISE as well as the flexibility of SPE and thus allowing for the fabrication of thin layers [126–128]. Nonetheless, they still suffer from poor interfacial contact. In recent years, the introduction of IL to CSEs has also received increased research interest. For example, the conductivity of the Li-salt-free polyethylene oxide (PEO) combined with $Li_{6.4}La_3Zr_{1.4}Ta_{0.6}O_{12}$ (LLZTO) CSE membrane increases by one order of magnitude when wetted with BMIMTFSI (IL). This enhancement has been attributed to the increased ion paths along with the IL-connected interfaces between the conductive polymer matrix and the SE particles, resulting in a much reduced interface resistance (Fig. 9a, b) [129]. Similarly, $Pyr_{13}TFSI$ with LiTFSI salt was added into PVDF-HFP/LAGP CSE system. The addition of ILE largely increased the ionic conductivity, with the optimal performance achieved for ILE content of 60 % [120]. Interestingly, the direct coating of the CSE paste on the lithium metal surface yielded to an excellent electrochemical performance [123], offering an option to further simplify the cell manufacturing process.

Notably, the impact of lithium salt concentration on electrolyte properties cannot be ignored, as in the case of high concentration liquid electrolytes that are capable of adjusting the ion solvation structure to regulate the electrolyte properties, such as the interfacial chemistry and ion transport [130–132]. A super concentrated ionogel-in-ceramic HE was proposed[121] through cohering the LLZO particles with a 3 M LiTFSI-EMIMFSI-PMMA ionogel (Fig. 9c). This specifically designed electrolyte enabled an ultra-high ionic conductivity of 1.33×10^{-3} S cm^{-1} at 25 °C (Fig. 9d) as well as a high lithium-ion transference number of 0.89, demonstrating a superior performance than the ionogel electrolyte. The high ionic conductivity and Li^+ transference number is closely associated to the lithium ion local environment and transport mechanism, which can be investigated via solid-state static nuclear magnetic resonance (NMR). As shown in Fig. 9e, a single ^7Li resonance peak was detected at -0.31 ppm in the ionogel sample, which is assigned to the LiTFSI component, a peak shift was found in the super-concentrated ionogel-in-ceramic (SIC) electrolyte that can be attributed to the de-coordination of $TFSI^-$ anion from Li cation. The much narrower peak suggests an enhancement of lithium-ion mobility in SIC electrolyte, owing to the interaction between LLZO surface and Li^+ mediated by the IL.

In summary, the introduction of IL in CSEs creates a liquid-phase bridge to connect polymer electrolyte and inorganic electrolyte, enhancing the ionic conductivity of CSEs. Moreover, the IL is beneficial to improve the viscoelasticity of CSEs reducing the interfacial resistance between electrodes and electrolyte. The IL could contribute to form a stable LiF-rich SEI layer on the LMA and suppress the growth of lithium dendrites. However, the complex lithium-ion transport at organic and inorganic interfaces necessitates further research as well as elucidation of the role of ILs especially in the ion transport mechanism. Hence, resolving the relevant ion transport pathway through the heterogenous hybrid CSEs is critical. Liu et al. [122] adopted solid-state NMR spectroscopy to examine the interface of PEO-Li_6PS_5Cl composite electrolyte. The sluggish lithium ion transport across organic/inorganic phase in CSEs was identified as the primary limiting factor, due to a fairly low lithium ion conductivity at the interface considering a deficiency of ethereal oxygen species and as well as the absence of local mobility (Fig. 10a). To improve the interface diffusivity, two different ILs (imidazole-based EMIMTFSI and piperidinium-based $PP_{13}TFSI$) were selected, which exhibit completely different miscibility in PEO matrix. They discovered that the miscible EMIMTFSI participated into PEO matrix and reduced the crystalline fraction, enhancing the conductivity of PEO. However, the less miscible $PP_{13}TFSI$ remained on the interface of Li_6PS_5Cl phase and enhanced the local mobility, which facilitated the

Table 3
Comparison of the performance of different ILs in hybrid electrolytes.

Types of ILs	Components of HEs	Ratio (wt.%)	Ionic conductivity	Cathode/Anode	Performance	Refs.
$Pyr_{14}TFSI$	LiTFSI/IL/TiO_2	53/2/45	1.5×10^{-3} S cm^{-1} (20 °C)	LFP/Li	89 % after 100 cycles at 0.1 C and RT	[117]
$Pyr_{14}TFSI$	LiTFSI/IL/LLZO	1/19/80	0.4×10^{-3} S cm^{-1} (25 °C)	LCO/Li	99 % after 150 cycles at 0.1 C and 25 °C	[118]
BMPTFSI	IL/LLZO	14/86	0.67×10^{-3} S cm^{-1} (20 °C)	NCM811/Li	68 % after 200 cycles at 0.5 C and 20 °C	[81]
$C_{10}mimBF_4$	Li_3GaF_6	-	10^{-4} S cm^{-1} (RT)	LFP/Li	69 % after 150 Cycles at .5 C and 60 °C	[119]
$Pyr_{13}TFSI$	LiTFSI/IL/LAGP/PVDF-HFP	40/17/6/37	1.23×10^{-3} S cm^{-1} (25 °C)	LFP/Li	86.3 % after 400 cycles at 1 C and 55 C	[120]
EMIFSI	LiTFSI/IL/PMMA/PEGDMA	-	1.33×10^{-3} S cm^{-1} (25 °C)	NCM523/Li	72.7 % after 200 cycles at 1 C and 25 °C	[121]
$PP_{13}TFSI$/EMITFSI	LiTFSI/IL/PEO/Li_6PS_5Cl	-	2.47×10^{-4} S cm^{-1} (RT)	LFP/Li	~82 % after 50 cycles at 0.18 C and 50 °C	[122]
BMIMTFSI	IL/PEO/LLZO-Sb	15/10/75	1.1×10^{-4} S cm^{-1} (25 °C)	NCM/Li	84.5 % after 100 cycles at 0.1 C and 25 °C	[123]

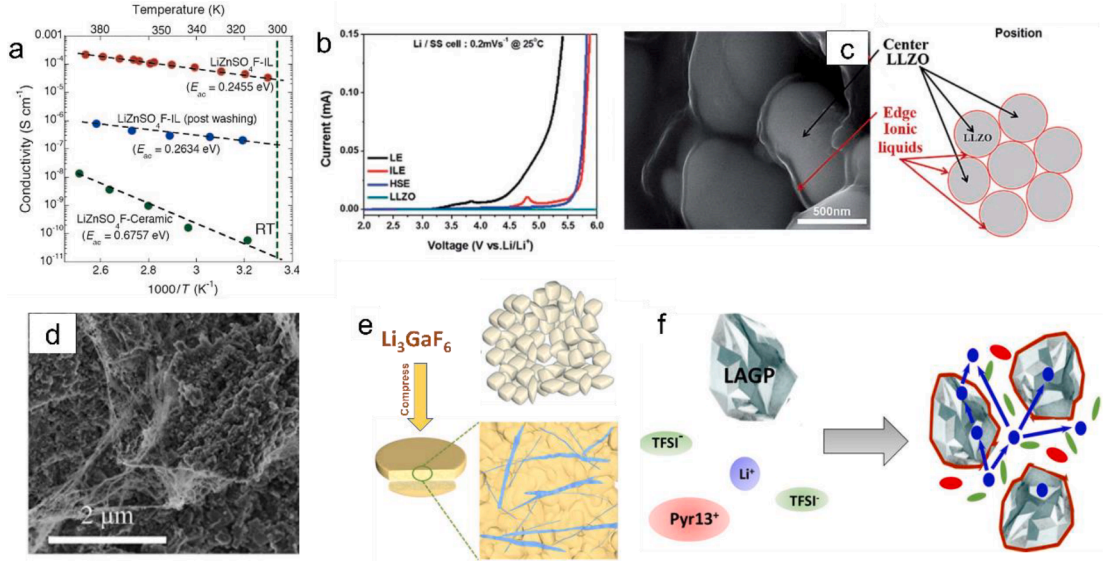

Fig. 8. (a) AC conductivity of ionically blocking $LiZnSO_4F$ pellets prepared using $ZnSO_4{\cdot}H_2O$ precursor made with and without ionic liquid. Reproduced with permission [76]. Copyright 2011, Wiley. (b) Linear sweep voltammetry for the Li/LE/SS, Li/ILE/SS, Li/HE/SS, and Li/LLZO/SS cells. (c) LLZO ceramic with the ionic liquid and the schematic illustration of a matrix formed by LLZO-ionic liquid (LiTFSI and $Py_{14}TFSI$). Reproduced with permission [118]. Copyright 2016, Royal Society of Chemistry. (d) Cross-sectional SEM images LGF pellet. (e) Schematic compressing processes of LGF powders into corresponding pellets, where solidified IL as *in-situ* binder can be extruded from fluoride grain boundaries. Reproduced with permission [119]. Copyright 2020, Elsevier. (f) Mechanism of cation exchange between $Pyr_{13}TFSI$ and LAGP at the surface of LAGP and the lithium diffusion pathway reaction at different current density. Reproduced with permission [125]. Copyright 2022, American Chemical Society.

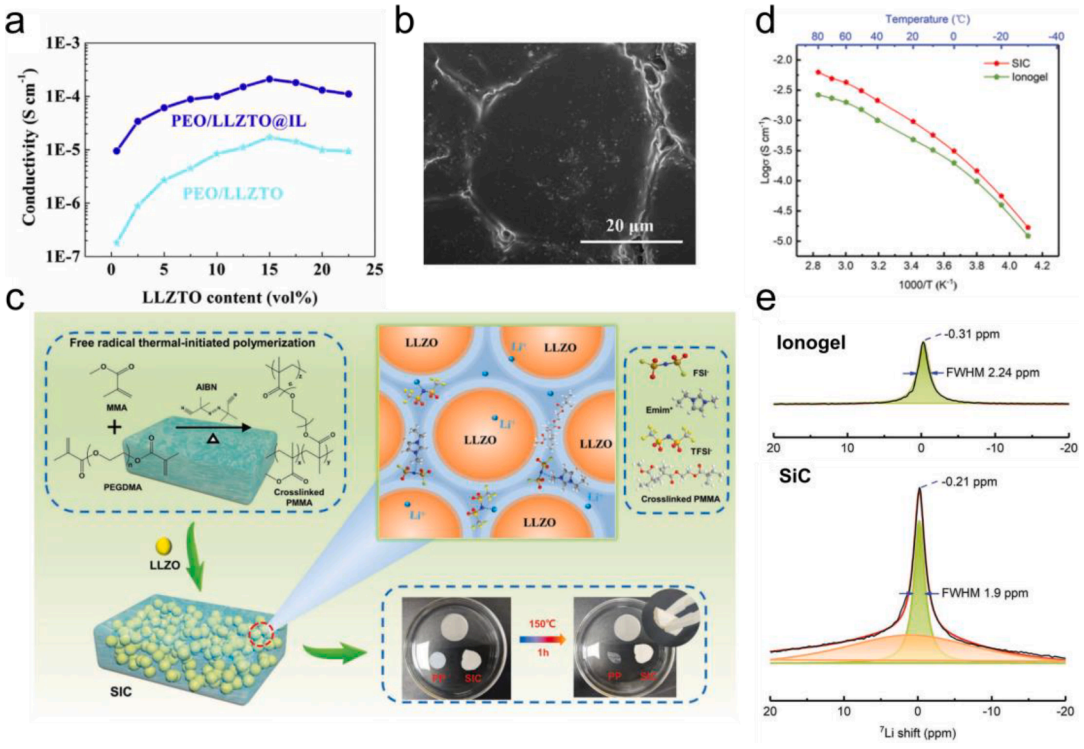

Fig. 9. (a) Ionic conductivity of PEO/LLZTO and PEO/LLZTO@IL with different content of LLZTO. (b) Plane-view SEM of 20 μm-thick PEO/LLZTO@IL. Reproduced with permission [129]. Copyright 2020, Elsevier. (c) Schematic illustration showing the *in situ* synthesis of the SIC electrolyte and the network of the SIC electrolyte. (d) Conductivity-temperature curves of SIC and ionogel. (e) Solid-state static ^7Li NMR spectra for ionogel electrolyte and, SIC electrolyte. Reproduced with permission [121]. Copyright 2022, Wiley.

lithium-ion transport over the organic/inorganic interface (Fig. 10c). This ion transport proceeded rather than transport only in the polymer phase without the utilization of high conductivity of the Li_6PS_5Cl phase (Fig. 10b), resulting in a higher overall conductivity of the hybrid PEO-Li_6PS_5Cl electrolyte with the assistance of $PP_{13}TFSI$.

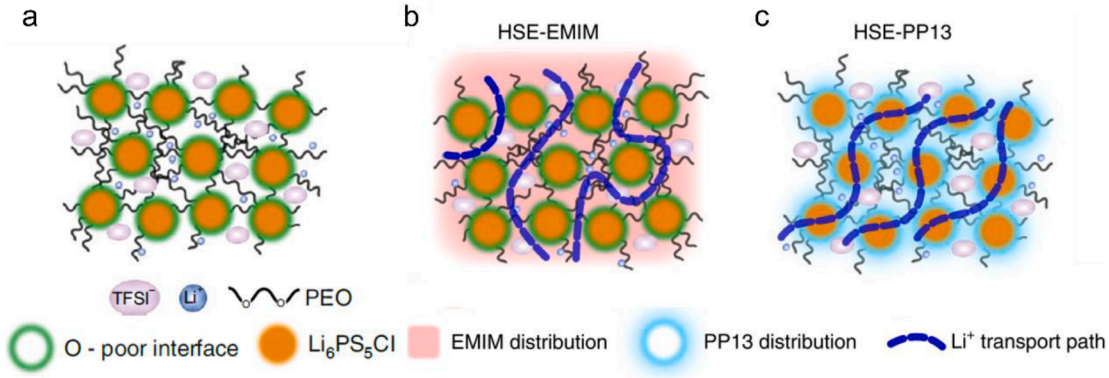

Fig. 10. (a) Schematic illustration of lithium-ion diffusion pathways in the HE. (b) Proposed mechanism for lithium-ion diffusion in HEs with EMIM-TFSI and PP_{13}TFSI IL additives. Reproduced with permission [122]. Copyright 2022, Nature.

3.3. IL serving as plasticizer for solid polymer electrolytes

ISEs generally possess a high stiffness and consequently a large interfacial resistance between SE and electrodes. In contrast, SPEs exhibit outstanding interfacial compatibility and superior flexibility [133,134]. Nonetheless, the inferior ionic conductivity remains one of the main challenges for polymer electrolytes. The addition of plasticizer, i.e., an additive increasing the mobility of the polymer chains [135], is regarded as an effective route to enhance the electrical properties of polymer electrolyte [70,136,137]. ILs were discovered to display a plasticizing effect on polymer electrolyte, contributing to a reduced crystalline phase of polymer matrix and enhanced segmental mobility, resulting in an improved ionic conductivity [138,139]. The IL-containing polymer electrolytes can be classified in two main types, SPEs and PILs. Depending on the function, they can also serve as sole electrolyte or as an effective interlayer. In this section, the role of ILs based on their functions as interfacial protecting layers for ISE and as sole SPEs are discussed. The performance of some typical works are summarized and compared in the Table 4.

3.3.1. Interlayer

The uncompacted interface caused by the rigidity of ISE is a crucial issue for all inorganic SSBs. Introducing a soft and flexible polymer interlayer would be an appropriate choice to fill the vacancies between SE and metal anode. IL is a good plasticizer for the preparation of a protective interlayer, considering its excellent ion mobility and thermal stability [146]. A simple approach was employed using IL to dissolve PEO to prepare a mixed coating layer on the Ga-doped LLZO [147], the coating layer can effectively enhance the physical contact between SE and lithium metal resulting in a reduced interfacial resistance. Nevertheless, severe capacity degradation was observed accompanying a fairly low Coulombic efficiency, demonstrating that the simple mixture is insufficient to protect the SE as an interlayer. This may be associated to an uneven amorphous phase of the polymer interlayer leading to a low ionic conductivity. Two promising approaches can be adopted to improve the performance of PEO/IL/Li-salts ternary system, one method is adding inorganic fillers, for example, $BaTiO_3$ was chosen as the filler to prepare a protecting SE film, combining PEO, LiTFSI and IL. The protected $Li_{1.4}Al_{0.4}Ge_{0.2}Ti_{1.4}(PO_4)_3$ (LAGTP) exhibited an excellent stability against lithium metal with a low polarization [148]. However, with this route it is still difficult to completely prevent the crystallization of PEO. Another method is the cross-linking of polymer matrix to form a stable fully amorphous phase. Recently, an ultrathin solid polymer interlayer was reported using PEO as the matrix which was cross linked with IL using benzophenone (BP) as the photo-initiator (Fig. 11a) [111], the thin polymer interlayer with high ionic conductivity effectively protected the interface between NASICON-type LAGP and lithium metal, restrained the reduction of Ge^{4+} as well as suppressed the growth of lithium dendrites (Fig. 11b). This outstanding interlayer enables a good cycling stability with a capacity retention of 83 % after 400 cycles at 0.2 C accompanying a high average Coulombic efficiency of 99.96 %. Apart from the preparation of a special polymer film as the interlayer, a more facile strategy for the preparation of an interlayer was proposed via directly mixing LAGP nanoparticles with ILE to obtain a quasi-solid-state paste (Fig. 11c)[82], the tailored multifunctional interlayer established a high stability interphase with a low resistance (5 Ω cm^2) and long-term interfacial chemical stability for 1500 h (Fig. 11d), and achieved a high cycling stability with slight capacity fading of 0.053 % per cycle for 200 cycles. Recently, a conformal sericin protein film was employed to stabilize the LATP/Li interface. The electrochemically stable and electronically insulating interlayer effectively trapped and confined the IL as ion wires due to the intermolecular force between sericin-chain and TFSI anion group [142]. The designed interlayer suppressed the passivation and decomposition at the LATP/Li interface as well as reduced the cracks of LATP pellets. Additionally, *in-situ* polymerization [143] and drop-coating [140] techniques using ILs as the plasticizers were also applied to prepare the effective protecting interlayer between ISE and LMA. These new strategies offer routes to build a compact and durable interphase for the application of inorganic oxide ceramic electrolyte in lithium (and sodium) metal batteries.

3.3.2. IL-based solid polymer electrolyte

Interlayers using ILs as the plasticizer have demonstrated excellent performance to address the interfacial issues between ISE and metal

Table 4
The comparison of the performance of ILs served as plasticizer for solid polymer electrolytes.

Types of ILs	Components of Interlayer	Ratio (wt.%)	Ionic conductivity	Cathode/Anode	Performance	Refs.
Pyr13TFSI	LiTFSI/IL/PEGDA	15/85	0.5×10^{-4} S cm^{-1} (RT)	LFP/Li	91.5 % after 200 cycles at 0.5 C and 60 °C	[140]
VBIM-TFSI	LiTFSI/IL/Vinyl-PTMEG	-	3.18×10^{-5} S cm^{-1} (RT)	LFP/Li	92 % after 100 cycles at 0.5 C	[141]
Pyr_{13}TFSI	LiTFSI/IL/PVDF	14:46:40	3.91×10^{-4} S cm^{-1} (RT)	LCO/Li	85.9 % after 100 cycles at 0.2C and RT	[142]
$VEImNTF_2$	LLZTO/TPGDA/IL	-	6.9×10^{-4} S cm^{-1} (25 °C)	LFP/Li	88.3 % after 600 cycles at 0.5 C and 0 °C	[143]
BMIMFSI	IL/LAGP	50/50	10^{-3} S cm^{-1} (30 °C)	LFP/Li	89.4 % after 200 cycles at 0.3 C and RT	[82]
HACC-TFSI	LiTFSI/PEO/HACC-TFSI	22/69/9	1.77×10^{-5} S cm^{-1} (30 °C)	LFP/Li	~97 % after 100 cycles at 0.2 C and 60 °C	[144]
EMIMTFSI	PAN@ZIF/IL	-	8.17×10^{-4} S cm^{-1} (RT)	NCM811/Li	95.3 % after 500 cycles at 1 C and 25 °C	[145]

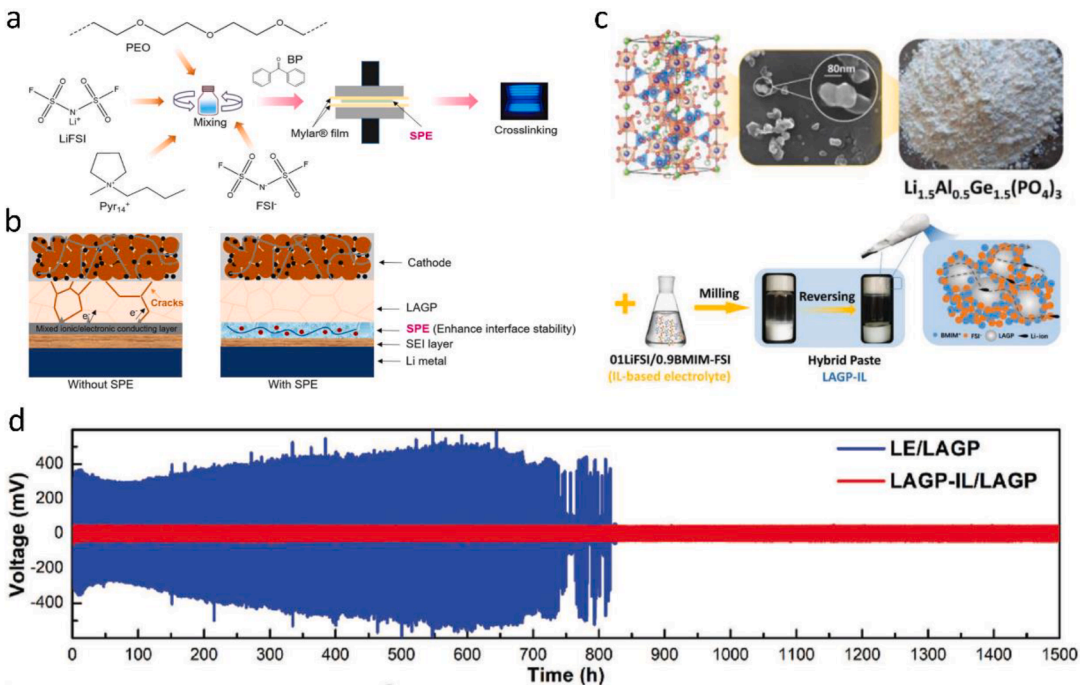

Fig. 11. (a) Preparation of the SPE interlayer for QSSBs and (b) schematic illustration of Li|LAGP|NCM811 QSSBs without and with the SPE interlayer. Reproduced with permission [111]. Copyright 2023, Elsevier. (c) Schematic diagram of preparation of LAGP-IL hybrid paste. (d) Voltage profiles of Li|LAGP pellet|Li symmetric cells with a LAGP-IL interlayer or a liquid electrolyte (LE, 1 m $LiPF_6$ in EC/DEC) to wet the interface, operating at a current density of 0.1 mA cm^{-2} and a capacity density of 0.1 mAh cm^{-2}. Reproduced with permission [82]. Copyright 2020, Wiley.

anode, however, the poor interface contact between cathode and SE remains. Therefore, polymer electrolytes containing IL were also employed as the sole SE. The introduction of ILs in "polymer-in-salt" electrolyte system dates back to 1995 [149]. Since then, numerous works have emerged focused on the development of the physical and chemical properties of IL-containing polymer electrolytes [71,98,150,151]. ILs are of mainly two different types in polymer electrolytes, SPE with PEO and others as the matrix or poly(ionic liquid) (PILs). Previous literatures have reviewed the early works in detail [146,152,153], therefore recent advancements in the field are reported here.

First, PEO-based polymer system is restrained by the low transference number, high degree of crystallinity and inferior high voltage stability [134,154]; a series of solutions were employed to resolve these drawbacks. For example, targeting the low transference number of PEO-based SPE at ambient temperature (0.1-0.2), a PEO-like structure of polytetramethylene ether glycol (PTMEG) was used to replace PEO matrix. When combined with 1-vinyl-3-butylimidazole bis(trifluoromethanesulfonyl)imide (VBIM-TFSI) IL, a higher transference number of up to 0.47, a wide ESW (> 5 V) as well as good interface compatibility were obtained [141]. This improvement is attributed to

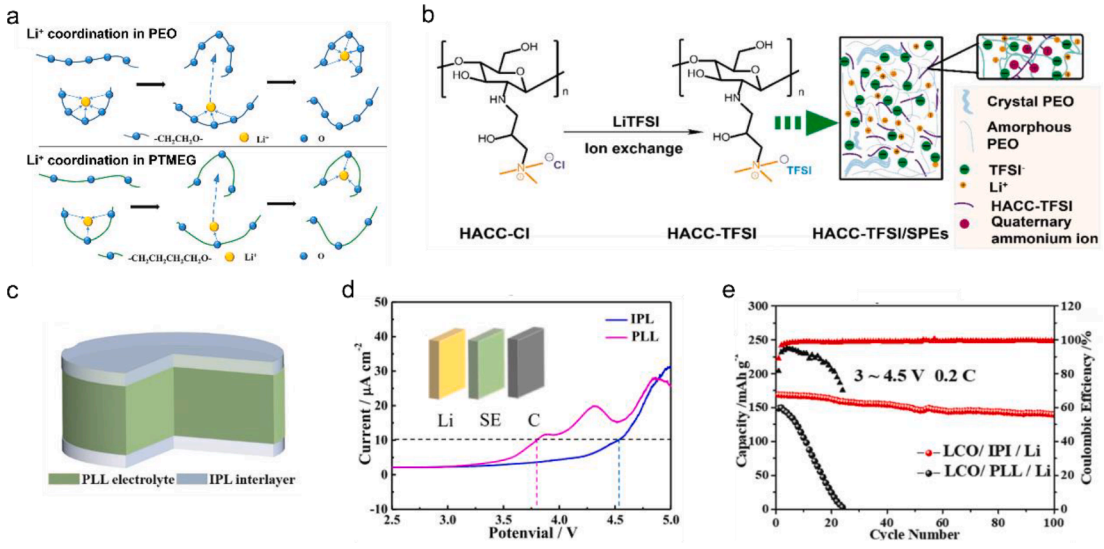

Fig. 12. (a) Schematic illustration of the loose coordination structure of PTMEG compared to PEO. Reproduced with permission [141]. Copyright 2021, Elsevier. (b) Synthetic scheme of HACC-TFSI/SPEs. Reproduced with permission [144]. Copyright 2020, Elsevier. (c) Schematic diagram of PEO-based electrolyte with IL-containing PVDF-HFP-based electrolyte (IPL) interlayer. (d) Linear sweep voltammetry curves of IPL and PEO-LLZTO (PLL) electrolyte using Li/electrolyte/carbon cells. (e) Cycling behavior of the cells at 0.2C and a high cut-off voltage up to 4.5 V. Reproduced with permission [142]. Copyright 2021, Elsevier.

facile lithium coordination and dissociation due to a weaker Li^+-O interaction compared to pure PEO system (Fig. 12a). The designed SPE enabled a good cycling stability with a capacity retention of 92 % after 100 cycles in the Li/SPE/$LiFePO_4$ cells at ambient temperature. With respect to the high degree of crystallinity and poor ionic conductivity, a hydroxypropyl trimethylammonium bis(trifluoromethanesulfonyl) imide chitosan salt (HACC-TFSI) was used to increase the amorphous region, the interaction between quaternary cations and TFSI anions contributed to the Li^+ dissociation and thus the enhanced ion mobility (Fig. 12b) [144]. In addition, the poor oxidation resistivity of PEO-based electrolyte towards high voltage cathode ($\geq$ 4.3 V) was also improved, through designing a poly(vinylidene-di-fluoride-hexafluoropropylene) (PVDF-HFP)-based electrolyte containing IL to resolve the issue of high voltage PEO-based SSB. When the mixture of PVDF-HFP and IL was employed as the interlayer in PEO-based solid state cells (Fig. 12c), a higher ESW was obtained (Fig. 12d), inducing a superior cycling stability at the high cut-off voltage of 4.5 V (Fig. 12e) [142].

PILs display a high chemical stability and thermal stability, along with a wide electrochemical window (up to 5 V) [152,155]. However, the inferior mechanical properties hinder its further development as well as the difficulty to suppress the growth of lithium dendrites resulting in cell failure and even safety issues. Enhancement of the modulus value of PILs is a critical challenge for the application of PILs. Recently, ethylene carbonate (EC) was chosen as a cosolvent to combine with poly(styrene-b-1-((2-acryloyloxy)ethyl)-3-butylimidazolium bis (tri-fluoromethanesulfonyl)imide) and LiFSI to prepare a polymerized IL block copolymer film. The introduction of EC decreased the glass transition temperature (T_g) of PILs and increased the ionic conductivity. The optimal mechanical stability of the polymer film was achieved with an EC/LiFSI molar ratio of ~2 [156]. Unsatisfactory ionic conductivity is another issue that must be resolved to compete with commercial electrolytes. Hu et al. designed a PIL through high-charge density polymerized ionic networks which obtained a fairly high ionic conductivity of 5.89×10^{-3} S cm^{-1} and achieved high cycling stability in full cells [157]. Considering that the role of PILs as polyelectrolytes in batteries has been already summarized in a few recent reviews [152,155,158], the focus here is given to the application of ILs at the interfaces of SSBs.

3.4. *Effect of ILs on the structure of electrodes or SE*

Battery electrodes generally face certain volume change upon repeated Li^+/Na^+ uptake and release, which results in the poor interfacial contact between electrodes and SEs. Here, ILs may act a soft buffer to offset the detrimental effect from electrodes' volume change. However, the cracking phenomena is another knotty issue for the SSBs, occurring in the electrodes or SEs. Regarding to cathodes, some ILs were reported to effectively restrain the generation of microcracks in liquid electrolyte-based lithium metal batteries, preventing phase transitions in Ni-rich materials by forming highly stable CEI layer [60]. EMI-based ILs incorporated in $LiCoO_2$ composite cathodes for SSB did not prevent the active material particles' cracking because of the non-performing (i.e., continuously growing) CEI layer (Fig. 13a,b), resulting in the gradual performance decay. This failure was associated to the low electrochemical stability of EMI-based ILs being only slightly higher than 4 V vs. Li/Li^+. Nonetheless, the IL reduced the cracks or voids when employed as an interlayer (Fig. 13c,d), avoiding the subsequent inhomogeneous metal deposition and dendrites formation. This is particularly true for NASICON-type SEs, which high reactivity with LMA result in the occurrence of inside-the-particle-stress, mechanical degradation, and, eventually, generation of cracks [159]. Although the IL does not suppress the cracking of NASICON-type SEs, a conformal sericin interlayer, confining the IL near the SE's particles, mitigates the cracking phenomenon and the dendritic Li growth upon long-term cycling (Fig. 13e) [159]. Similarly, a LAGP-IL hybrid interlayer was found to reduce the SE's cracks upon cell cycling (Fig. 13f–i) [82]

4. Summary and outlook

Interface engineering is the primary focus for the further development of solid-state battery technologies. Rational design and regulation of the interfaces between electrodes and electrolytes are required to establish a practical SSB system. The remarkable properties of nonflammability, fluidity and voltage resistance enable ILs to play crucial roles in modifying the interfacial engineering of SEs. The applications of ILs in SSBs are mainly divided into four different types: liquid additive as the interfacial wetting agent, hybrid electrolyte mixing with ISEs, PILs, and plasticizer in SPE. Currently, there is a lack of systematic, in-depth investigations of ILs in (quasi) solid state batteries.

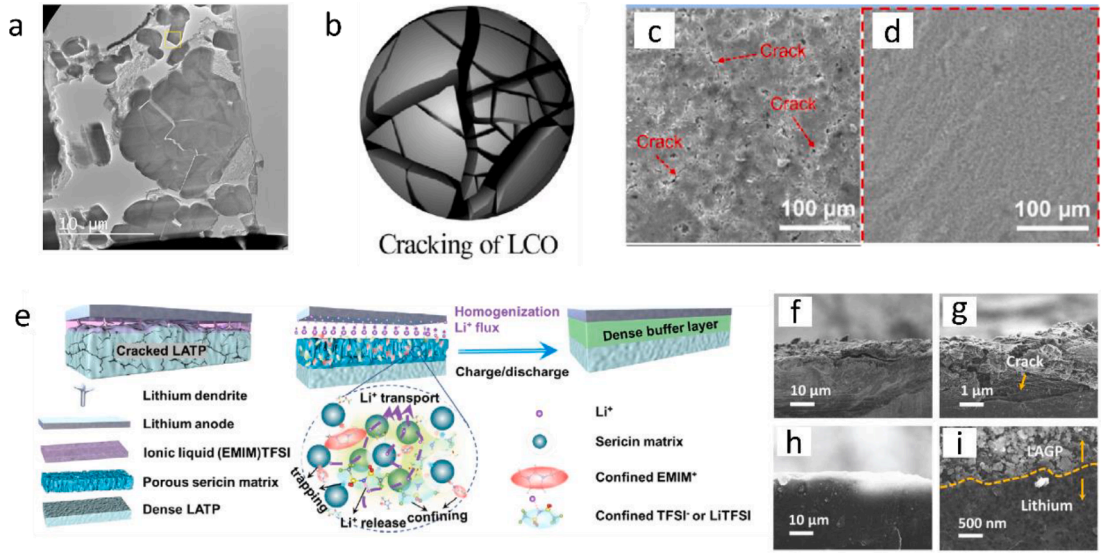

Fig. 13. (a) The IL-containing composite cathode cycled after 100 cycles at 60 °C [87]. (b) The sketch map of cracking LCO caused by stress accumulation and fatigue [87]. SEM micrographs of the Na_3SbS_4 SE without (c) and with (d) IL interlayer [91]. (e) Schematic diagram of interface environment of Li/LATP without (left) and with (right) IL-based interlayer [159]. Morphology of cycled LMA using liquid electrolyte wetter in (f) low magnification and (g) high magnification and using LAGP-IL interlayer in (h) low magnification and (i) high magnification.

Furthermore, the key factors that must be considered for the practical realization of these systems in the near future are presented.

4.1. Interfacial wetting agent

This approach is a simple but effective interface engineering method, in which the ILs work as a "lube" to enhance the interfacial ions transport. First, the further study of ILs on thin membrane SEs are encouraged instead of pressed pellet-type SEs. Hence, a vital challenge for current ISEs is the preparation of thin membranes, especially for oxide-type SEs. Developing CSEs could be a solution for the preparation of thin membranes, nevertheless, the introduction of complicated multiphases would affect the function of ILs at the interfaces of CSEs compared to pure ISEs. Second, previous research has demonstrated that the ILs utilized as the wetting agent on LMA side are dependent on the SEs type. For example, ILs are highly effective in suppressing lithium dendrites and enhancing the contact between garnet-type SE and LMA. Nevertheless, similar functions are absent in NASICON-type SEs due to the severe reduction reactions. Beside SEs types, the properties of ILs should also be considered. For example, the cation type influences the compatibility with lithium (sodium) metal, salt concentration effects the ionic conductivity, viscosity and ion transference number of ILs. Employing ILs as interfacial wetter enhances the physical contact between electrodes and SE, eliminating the bottleneck of ion transport in the SSBs.

4.2. Hybrid electrolytes

HEs (including CSEs) combine the advantages of fluidity from IL and mechanical strength from the inorganic component or even flexibility from polymer component and can be easily fabricated as thin electrolyte membranes. Meanwhile, the HEs have superior contact with electrodes, especially at the anode side. Soon, resolving the complex ion transport mechanisms at the interfaces between multiple components in HEs is an important direction that requires study by advanced *in-situ*/operando techniques, such as solid-state NMR spectroscopy, theoretical simulations, and synchrotron characterizations. Understanding the ion transfer preference or barrier could in-turn benefit the design of high-performance HEs. To design satisfactory HEs, several factors need to be considered: *a*. The compatibility between ILs and SEs. The types of cations and anions in the IL strongly influence the miscibility, wettability, and compatibility of HEs. For example, the $PP_{13}TFSI$ has an inferior miscibility in PEO compared to EMIMTFSI. Therefore, the selection of IL is important to improve the properties of specified SE components. *b*. The ratio of salt/IL/SEs. The ratio among different components directly effects the physical and chemical properties of the membrane, and determines the type of electrolyte, i.e., all-solid-state, quasi-solid-state or even gel-state; high concentration IL-based solid-state battery systems require further study. *c*. The interfacial contact between HEs and electrodes needs to be considered as it can be affected by the ratio, hence, it should be well balanced when designing the HEs.

4.3. Solid polymer electrolytes

To utilize SPE as an interlayer, the SPE requires a good compatibility with lithium (sodium) metal anode, thus the IL should exhibit a low reduction potential below 0 V vs. Li/Li^+ (Na/Na^+). The more stable pyrrolidinium-based ILs can be considered for designing SPE. However, this bilayer SE configuration via an additional SPE would greatly increase the manufacturing complexity and cost. A simpler route through directly casting or *in situ* solidification on SEs or LMA (SMA) should be pursued, in addition, the thickness of the interlayer should be as thin as possible. For the utilization of IL as the sole polymer electrolyte, except for the compatibility against anode, the high voltage resistivity against cathode should be also balanced. Furthermore, the ionic conductivity and ions transference number are critical factors to be improved, developing single ion conducting polymer matrix as well as the introduction of inorganic fillers to immobilize the IL's cation and/or anion must be considered.

In summary, with the potential to play different roles in resolving the crucial interfacial issues of SSBs, ILs are promising materials for implementation in the SSB configuration. It should be emphasized that although ILs have been investigated in battery fields for many years, besides their high viscosity, the application of ILs in commercial batteries is also limited by their costliness and the lack of a compatible separator. However, the emerging SSB systems may provide a new platform for the application of ILs. On one hand, the unit amount of ILs would be reduced when being applied to SSBs, especially if used as the wetting agent or thin interlayer, which drastically decreases the overall cost of ILs. On the other hand, the ISE in HE or polymer matrix in SPE could act as a separator. As a result, the critical drawbacks of ILs could be well avoided in the application of SSB system, which works as a bit, but pivotal "grease" to lubricate the SEs/electrode interface.

CRediT authorship contribution statement

Fanglin Wu: Conceptualization, Writing – original draft, Writing – review & editing. **Zhen Chen:** Conceptualization, Writing – review & editing. **Shan Fang:** Writing – original draft, Funding acquisition, Writing – review & editing. **Wenhua Zuo:** Writing – review & editing. **Guk-Tae Kim:** . **Stefano Passerini:** Conceptualization, Funding acquisition, Resources, Supervision, Writing – review & editing.

Declaration of Competing Interest

The authors declare that they have no known competing financial interests or personal relationships that could have appeared to influence the work reported in this paper.

Data availability

No data was used for the research described in the article.

Acknowledgments

The authors would like to acknowledge financial support from the projects funded by the National Natural Science Foundation of China (52002176, 52161039), Jiangxi Provincial Natural Science Foundation (20212BAB214054), National Research Foundation of Korea(NRF) grant funded by the Korea government(MSIT)(No. RS-2023-00217581)). S.P. acknowledges the basic funding of Helmholtz Association.

References

[1] L. Chen, G. Msigwa, M. Yang, A.I. Osman, S. Fawzy, D.W. Rooney, P.S. Yap, Strategies to achieve a carbon neutral society: a review, Environ. Chem. Lett. 20 (2022) 2277–2310.
[2] M.J. Haensgen, A.M. Lechner, S. Rakotonarivo, P. Leepreecha, M. Sakboon, T. W. Chu, E. Auclair, I. Vlaev, Implementation of the COP26 declaration to halt forest loss must safeguard and include Indigenous people, Nat. Ecol. Evol. 6 (2022) 235–236.
[3] W. Wu, W. Luo, Y. Huang, Less is more: a perspective on thinning lithium metal towards high-energy-density rechargeable lithium batteries, Chem. Soc. Rev. 52 (2023) 2553–2572.
[4] H. Su, Z. Chen, M. Li, P. Bai, Y. Li, X. Ji, Z. Liu, J. Sun, J. Ding, M. Yang, X. Yao, C. Mao, Y. Xu, Achieving practical high-energy-density lithium-metal batteries by a dual-anion regulated electrolyte, Adv. Mater. (2023), e2301171, https://doi.org/10.1002/adma.202301171.
[5] L.Z. Fan, H. He, C.-W. Nan, Tailoring inorganic–polymer composites for the mass production of solid-state batteries, Nat. Rev. Mater. 6 (2021) 1003–1019.
[6] J. Li, F. Li, L. Zhang, H. Zhang, U. Lassi, X. Ji, Recent applications of ionic liquids in quasi-solid-state lithium metal batteries, Green Chem. Eng. 2 (2021) 253–265.
[7] H. Huo, J. Janek, Solid-state batteries: from 'all-solid' to 'almost-solid', Natl. Sci. Rev. 10 (2023) nwad098.

[8] Z. Chang, H. Yang, X. Zhu, P. He, H. Zhou, A stable quasi-solid electrolyte improves the safe operation of highly efficient lithium-metal pouch cells in harsh environments, Nat. Commun. 13 (2022).

[9] D. Wu, F. Wu, Toward better batteries: Solid-state battery roadmap 2035+, eTransportation 16 p. 2023.

[10] K.J. Kim, M. Balaish, M. Wadaguchi, L. Kong, J.L.M. Rupp, Solid-state Li–metal batteries: challenges and horizons of oxide and sulfide solid electrolytes and their interfaces, Adv. Energy Mater. 11 (2020) 2002689.

[11] A.M. Bates, Y. Preger, L. Torres-Castro, K.L. Harrison, S.J. Harris, J. Hewson, Are solid-state batteries safer than lithium-ion batteries? Joule 6 (2022) 742–755.

[12] F. Wu, G.T. Kim, M. Kuenzel, H. Zhang, J. Asenbauer, D. Geiger, U. Kaiser, S. Passerini, Elucidating the effect of iron doping on the electrochemical performance of cobalt-free lithium-rich layered cathode materials, Adv. Energy Mater. 9 (2019) 1902445.

[13] M. Kuenzel, G.T. Kim, M. Zarrabeitia, S.D. Lin, A.R. Schuer, D. Geiger, U. Kaiser, D. Bresser, S. Passerini, Crystal engineering of TMPOx-coated LiNi0.5Mn1.5O4 cathodes for high-performance lithium-ion batteries, Mater. Today 39 (2020) 127–136.

[14] Y. Kato, S. Hori, T. Saito, K. Suzuki, M. Hirayama, A. Mitsui, M. Yonemura, H. Iba, R. Kanno, High-power all-solid-state batteries using sulfide superionic conductors, Nat. Energy 1 (2016).

[15] Y. Lu, L. Li, Q. Zhang, Z. Niu, J. Chen, Electrolyte and interface engineering for solid-state sodium batteries, Joule 2 (2018) 1747–1770.

[16] X. Miao, H. Wang, R. Sun, C. Wang, Z. Zhang, Z. Li, L. Yin, Interface engineering of inorganic solid-state electrolytes for high-performance lithium metal batteries, Energy. Environ. Sci. 13 (2020) 3780–3822.

[17] A. Banerjee, X. Wang, C. Fang, E.A. Wu, Y.S. Meng, Interfaces and interphases in all-solid-state batteries with inorganic solid electrolytes, Chem. Rev. 120 (2020) 6878–6933.

[18] L. Xu, S. Tang, Y. Cheng, K. Wang, J. Liang, C. Liu, Y.-C. Cao, F. Wei, L. Mai, Interfaces in solid-state lithium batteries, Joule 2 (2018) 1991–2015.

[19] J. Haruyama, K. Sodeyama, L. Han, K. Takada, Y. Tateyama, Space–charge layer effect at interface between oxide cathode and sulfide electrolyte in all-solid-state lithium-ion battery, Chem. Mater. 26 (2014) 4248–4255.

[20] M.W. Swift, Y. Qi, First-principles prediction of potentials and space-charge layers in all-solid-state batteries, Phys. Rev. Lett. 122 (2019) 167701.

[21] Y. Zhu, X. He, Y. Mo, First principles study on electrochemical and chemical stability of solid electrolyte–electrode interfaces in all-solid-state Li-ion batteries, J. Mater. Chem. A 4 (2016) 3253–3266.

[22] W.D. Richards, L.J. Miara, Y. Wang, J.C. Kim, G. Ceder, Interface stability in solid-state batteries, Chem. Mater. 28 (2016) 266–273.

[23] S.K. Jung, H. Gwon, S.S. Lee, H. Kim, J.C. Lee, J.G. Chung, S.Y. Park, Y. Aihara, D. Im, Understanding the effects of chemical reactions at the cathode–electrolyte interface in sulfide based all-solid-state batteries, J. Mater. Chem. A 7 (2019) 22967–22976.

[24] G.L. Gregory, H. Gao, B. Liu, X. Gao, G.J. Rees, M. Pasta, P.G. Bruce, C. K. Williams, Buffering volume change in solid-state battery composite cathodes with CO(2)-derived block polycarbonate ethers, J. Am. Chem. Soc. 144 (2022) 17477–17486.

[25] C. Yuan, W. Lu, J. Xu, Electrochemical-mechanical coupling failure mechanism of composite cathode in all-solid-state batteries, Energy Storage Mater. (2023) 102834.

[26] P. Minnmann, F. Strauss, A. Bielefeld, R. Ruess, P. Adelhelm, S. Burkhardt, S. L. Dreyer, E. Trevisanello, H. Ehrenberg, T. Brezesinski, F.H. Richter, J. Janek, Designing cathodes and cathode active materials for solid-state batteries, Adv. Energy Mater. 12 (2022).

[27] Y. Tian, Y. Sun, D.C. Hannah, Y. Xiao, H. Liu, K.W. Chapman, S.H. Bo, G. Ceder, Reactivity-guided interface design in Na metal solid-state batteries, Joule 3 (2019) 1037–1050.

[28] X.B. Cheng, C.Z. Zhao, Y.X. Yao, H. Liu, Q. Zhang, Recent advances in energy chemistry between solid-state electrolyte and safe lithium-metal anodes, Chem 5 (2019) 74–96.

[29] S. Wang, H. Xu, W. Li, A. Dolocan, A. Manthiram, Interfacial chemistry in solid-state batteries: formation of interphase and its consequences, J. Am. Chem. Soc. 140 (2018) 250–257.

[30] X. Han, Y. Gong, K.K. Fu, X. He, G.T. Hitz, J. Dai, A. Pearse, B. Liu, H. Wang, G. Rubloff, Y. Mo, V. Thangadurai, E.D. Wachsman, L. Hu, Negating interfacial impedance in garnet-based solid-state Li metal batteries, Nat. Mater. 16 (2017) 572–579.

[31] C. Wang, Y. Gong, B. Liu, K. Fu, Y. Yao, E. Hitz, Y. Li, J. Dai, S. Xu, W. Luo, E. D. Wachsman, L. Hu, Conformal, Nanoscale ZnO surface modification of garnet-based solid-state electrolyte for lithium metal anodes, Nano Lett. 17 (2017) 565–571.

[32] Y. Liu, Q. Sun, Y. Zhao, B. Wang, P. Kaghazchi, K.R. Adair, R. Li, C. Zhang, J. Liu, L.Y. Kuo, Y. Hu, T.K. Sham, L. Zhang, R. Yang, S. Lu, X. Song, X. Sun, Stabilizing the interface of NASICON solid electrolyte against Li metal with atomic layer deposition, ACS Appl. Mater. Interfaces 10 (2018) 31240–31248.

[33] Q. Liu, Q. Yu, S. Li, S. Wang, L. Zhang, B. Cai, D. Zhou, B. Li, Safe LAGP-based all solid-state Li metal batteries with plastic super-conductive interlayer enabled by in-situ solidification, Energy Storage Mater. 25 (2020) 613–620.

[34] Q. Yu, D. Han, Q. Lu, Y.B. He, S. Li, Q. Liu, C. Han, F. Kang, B. Li, Constructing effective interfaces for Li1.5Al0.5Ge1.5(PO4)3 pellets to achieve room-temperature hybrid solid-state lithium metal batteries, ACS Appl. Mater. Interfaces 11 (2019) 9911–9918.

[35] S. Fang, F. Wu, S. Zhao, M. Zarrabeitia, G.-T. Kim, J.-K. Kim, N. Zhou, S. Passerini, Adaptive multi-site gradient adsorption of siloxane-based protective layers enable high performance lithium-metal batteries, Adv. Energy Mater. n/a (2023) 2302577.

[36] A. Best, A. Bhatt, A. Hollenkamp, Ionic liquids with the bis (fluorosulfonyl) imide anion: electrochemical properties and applications in battery technology, J. Electrochem. Soc. 157 (2010) A903.

[37] Q. Yang, Z. Zhang, X.G. Sun, Y.S. Hu, H. Xing, S. Dai, Ionic liquids and derived materials for lithium and sodium batteries, Chem. Soc. Rev. 47 (2018) 2020–2064.

[38] S.A. Forsyth, J.M. Pringle, D.R. MacFarlane, Ionic liquids—an overview, Aust. J. Chem. 57 (2004) 113–119.

[39] J. Dupont, From molten salts to ionic liquids: a “nano” journey, Acc. Chem. Res. 44 (2011) 1223–1231.

[40] M. Armand, F. Endres, D.R. MacFarlane, H. Ohno, B. Scrosati, Ionic-liquid materials for the electrochemical challenges of the future, Nat. Mater. 8 (2009) 621–629.

[41] D.R. MacFarlane, M. Forsyth, P.C. Howlett, M. Kar, S. Passerini, J.M. Pringle, H. Ohno, M. Watanabe, F. Yan, W. Zheng, S. Zhang, J. Zhang, Ionic liquids and their solid-state analogues as materials for energy generation and storage, Nat. Rev. Mater. 1 (2016).

[42] K. Liu, Z. Wang, L. Shi, S. Jungsuttiwong, S. Yuan, Ionic liquids for high performance lithium metal batteries, J. Energy Chem. 59 (2021) 320–333.

[43] P.G. Balakrishnan, R. Ramesh, T. Prem Kumar, Safety mechanisms in lithium-ion batteries, J. Power Sources 155 (2006) 401–414.

[44] M. Egashira, M. Tanaka-Nakagawa, I. Watanabe, S. Okada, J.-i. Yamaki, Charge–discharge and high temperature reaction of $LiCoO_2$ in ionic liquid electrolytes based on cyano-substituted quaternary ammonium cation, J. Power Sources 160 (2006) 1387–1390.

[45] H. Sakaebe, H. Matsumoto, K. Tatsumi, Application of room temperature ionic liquids to Li batteries, Electrochim. Acta 53 (2007) 1048–1054.

[46] Y. Wang, K. Zaghib, A. Guerfi, F.F.C. Bazito, R.M. Torresi, J.R. Dahn, Accelerating rate calorimetry studies of the reactions between ionic liquids and charged lithium ion battery electrode materials, Electrochim. Acta 52 (2007) 6346–6352.

[47] Y. Takeda, O. Yamamoto, N. Imanishi, Lithium dendrite formation on a lithium metal anode from liquid, polymer and solid electrolytes, Electrochemistry 84 (2016) 210–218.

[48] H.E. Park, C.H. Hong, W.Y. Yoon, The effect of internal resistance on dendritic growth on lithium metal electrodes in the lithium secondary batteries, J. Power Sources 178 (2008) 765–768.

[49] A. Basile, A.I. Bhatt, A.P. O’Mullane, Stabilizing lithium metal using ionic liquids for long-lived batteries, Nat. Commun. 7 (2016) ncomms11794.

[50] D.J. Yoo, K.J. Kim, J.W. Choi, The synergistic effect of cation and anion of an ionic liquid additive for lithium metal anodes, Adv. Energy Mater. 8 (2018) 1702744.

[51] J.S. Wilkes, M.J. Zaworotko, Air and water stable 1-ethyl-3-methylimidazolium based ionic liquids, J. Chem. Soc. Chem. Commun. (1992), https://doi.org/10.1039/c39920000965.

[52] S. Brutti, E. Simonetti, M. De Francesco, A. Sarra, A. Paolone, O. Palumbo, S. Fantini, R. Lin, A. Falgayrat, H. Choi, M. Kuenzel, S. Passerini, G.B. Appetecchi, Ionic liquid electrolytes for high-voltage, lithium-ion batteries, J. Power Sources 479 (2020) 228791.

[53] B. Garcia, S. Lavallée, G. Perron, C. Michot, M. Armand, Room temperature molten salts as lithium battery electrolyte, Electrochim. Acta 49 (2004) 4583–4588.

[54] H. Sakaebe, H. Matsumoto, N-Methyl-N-propylpiperidinium bis (trifluoromethanesulfonyl)imide (PP13–TFSI) – novel electrolyte base for Li battery, Electrochem. Commun. 5 (2003) 594–598.

[55] J. Reiter, M. Nádherná, R. Dominko, Graphite and $LiCo_{1/3}Mn_{1/3}Ni_{1/3}O_2$ electrodes with piperidinium ionic liquid and lithium bis(fluorosulfonyl)imide for Li-ion batteries, J. Power Sources 205 (2012) 402–407.

[56] M. Galiński, A. Lewandowski, I. Stępniak, Ionic liquids as electrolytes, Electrochim. Acta 51 (2006) 5567–5580.

[57] W.Q. Feng, Y.H. Lu, Y. Chen, Y.W. Lu, T. Yang, Thermal stability of imidazolium-based ionic liquids investigated by TG and FTIR techniques, J. Therm. Anal. Calorim. 125 (2016) 143–154.

[58] N. Madria, T.A. Arunkumar, N.G. Nair, A. Vadapalli, Y.W. Huang, S.C. Jones, V. P. Reddy, Ionic liquid electrolytes for lithium batteries: Synthesis, electrochemical, and cytotoxicity studies, J. Power Sources 234 (2013) 277–284.

[59] J.F. Vélez, M.B. Vazquez-Santos, J.M. Amarilla, P. Tartaj, B. Herradón, E. Mann, C. del Río, E. Morales, Asymmetrical imidazolium-trialkylammonium room temperature dicationic ionic liquid electrolytes for Li-ion batteries, Electrochim. Acta 280 (2018) 171–180.

[60] F. Wu, S. Fang, M. Kuenzel, A. Mullaliu, J.-K. Kim, X. Gao, T. Diemant, G.T. Kim, S. Passerini, Dual-anion ionic liquid electrolyte enables stable Ni-rich cathodes in lithium-metal batteries, Joule 5 (2021) 2177–2194.

[61] V. Chaudoy, F. Ghamouss, J. Jacquemin, J.-C. Houdbert, F. Tran-Van, On the performances of ionic liquid-based electrolytes for Li-NMC batteries, J. Solution Chem. 44 (2015) 769–789.

[62] M. Barghamadi, A.S. Best, A.I. Bhatt, A.F. Hollenkamp, P.J. Mahon, M. Musameh, T. Rüther, Effect of $LiNO_3$ additive and pyrrolidinium ionic liquid on the solid electrolyte interphase in the lithium–sulfur battery, J. Power Sources 295 (2015) 212–220.

[63] J.-P. Hoffknecht, M. Drews, X. He, E. Paillard, Investigation of the N -butyl- N -methyl pyrrolidinium trifluoromethanesulfonyl- N -cyanoamide (PYR 14 TFSAM) ionic liquid as electrolyte for Li-ion battery, Electrochim. Acta 250 (2017) 25–34.

[64] T. Dong, L. Zhang, S. Chen, X. Lu, S. Zhang, A piperidinium-based ionic liquid electrolyte to enhance the electrochemical properties of $LiFePO_4$ battery, Ionics 21 (2015) 2109–2117.

[65] N. Bucher, S. Hartung, M. Arkhipova, D. Yu, P. Kratzer, G. Maas, M. Srinivasan, H. E. Hoster, A novel ionic liquid for Li ion batteries – uniting the advantages of guanidinium and piperidinium cations, RSC Adv. 4 (2014) 1996–2003.

[66] J.F. Vélez, M.B. Vázquez-Santos, J.M. Amarilla, B. Herradón, E. Mann, C. del Río, E. Morales, Geminal pyrrolidinium and piperidinium dicationic ionic liquid electrolytes. Synthesis, characterization and cell performance in $LiMn_2O_4$ rechargeable lithium cells, J. Power Sources 439 (2019).

[67] A. Warrington, L.A. O'Dell, O.E. Hutt, M. Forsyth, J.M. Pringle, Structure and interactions of novel ether-functionalised morpholinium and piperidinium ionic liquids with lithium salts, Energy Adv. 2 (2023) 530–546.

[68] G.A. Elia, U. Ulissi, S. Jeong, S. Passerini, J. Hassoun, Exceptional long-life performance of lithium-ion batteries using ionic liquid-based electrolytes, Energy Environ. Sci. 9 (2016) 3210–3220.

[69] F. Wu, G.T. Kim, T. Diemant, M. Kuenzel, A.R. Schür, X. Gao, B. Qin, D. Alwast, Z. Jusys, R.J. Behm, D. Geiger, U. Kaiser, S. Passerini, Reducing capacity and voltage decay of co-free $Li_{1.2}Ni_{0.2}Mn_{0.6}O_2$ as positive electrode material for lithium batteries employing an ionic liquid-based electrolyte, Adv. Energy Mater. 10 (2020) 2001830.

[70] D. MacFarlane, J. Sun, P. Meakin, P. Fasoulopoulos, J. Hey, M. Forsyth, Structure-property relationships in plasticized solid polymer electrolytes, Electrochim. Acta 40 (1995) 2131–2136.

[71] J. Shin, Ionic liquids to the rescue? Overcoming the ionic conductivity limitations of polymer electrolytes, Electrochem. Commun. 5 (2003) 1016–1020.

[72] J.H. Shin, W.A. Henderson, S. Passerini, An elegant fix for polymer electrolytes, Electrochem. Solid State Lett. 8 (2005) A125.

[73] J.H. Shin, W.A. Henderson, S. Passerini, PEO-based polymer electrolytes with ionic liquids and their use in lithium metal-polymer electrolyte batteries, J. Electrochem. Soc. 152 (2005) A978.

[74] G.B. Appetecchi, G.T. Kim, M. Montanino, M. Carewska, R. Marcilla, D. Mecerreyes, I. De Meatza, Ternary polymer electrolytes containing pyrrolidinium-based polymeric ionic liquids for lithium batteries, J. Power Sources 195 (2010) 3668–3675.

[75] F. Wu, G. Tan, R. Chen, L. Li, J. Xiang, Y. Zheng, Novel solid-state $Li/LiFePO_4$ battery configuration with a ternary nanocomposite electrolyte for practical applications, Adv. Mater. 23 (2011) 5081–5085.

[76] P. Barpanda, J.N. Chotard, C. Delacourt, M. Reynaud, Y. Filinchuk, M. Armand, M. Deschamps, J.M. Tarascon, LiZnSO4F made in an ionic liquid: a ceramic electrolyte composite for solid-state lithium batteries, Angew. Chem. 50 (2011) 2526–2531.

[77] K. Kerman, A. Luntz, V. Viswanathan, Y.-M. Chiang, Z. Chen, Review—practical challenges hindering the development of solid state Li ion batteries, J. Electrochem. Soc. 164 (2017) A1731–A1744.

[78] C.Z. Zhao, B.C. Zhao, C. Yan, X.Q. Zhang, J.-Q. Huang, Y. Mo, X. Xu, H. Li, Q. Zhang, Liquid phase therapy to solid electrolyte–electrode interface in solid-state Li metal batteries: a review, Energy Storage Mater. 24 (2020) 75–84.

[79] S.A. Pervez, G. Kim, B.P. Vinayan, M.A. Cambaz, M. Kuenzel, M. Hekmatfar, M. Fichtner, S. Passerini, Overcoming the interfacial limitations imposed by the solid-solid interface in solid-state batteries using ionic liquid-based interlayers, Small 16 (2020), e2000279.

[80] J.-Y. Wu, S.-G. Ling, Q. Yang, H. Li, X.-X. Xu, L.Q. Chen, Forming solid electrolyte interphase *in situ* in an ionic conducting $Li_{1.5}Al_{0.5}Ge_{1.5}(PO_4)_3$-polypropylene (PP) based separator for Li-ion batteries, Chin. Phys. B 25 (2016).

[81] Z. Zhang, L. Zhang, Y. Liu, H. Wang, C. Yu, H. Zeng, L.M. Wang, B. Xu, Interface-engineered Li_7 La_3 Zr_2 O_{12} -based garnet solid electrolytes with suppressed Li-dendrite formation and enhanced electrochemical performance, ChemSusChem 11 (2018) 3774–3782.

[82] S. Xiong, Y. Liu, P. Jankowski, Q. Liu, F. Nitze, K. Xie, J. Song, A. Matic, Design of a multifunctional interlayer for NASCION-based solid-state Li metal batteries, Adv. Funct. Mater. 30 (2020) 2001444.

[83] Z. Zhang, Q. Zhang, J. Shi, Y.S. Chu, X. Yu, K. Xu, M. Ge, H. Yan, W. Li, L. Gu, Y.-S. Hu, H. Li, X.-Q. Yang, L. Chen, X. Huang, A self-forming composite electrolyte for solid-state sodium battery with ultralong cycle life, Adv. Energy Mater. 7 (2017).

[84] Z. Bi, N. Zhao, L. Ma, Z. Fu, F. Xu, C. Wang, X. Guo, Interface engineering on cathode side for solid garnet batteries, Chem. Eng. J. 387 (2020).

[85] Q. Zhang, K. Pan, M. Jia, X. Zhang, L. Zhang, H. Zhang, S. Zhang, Ionic liquid additive stabilized cathode/electrolyte interface in $LiCoO_2$ based solid-state lithium metal batteries, Electrochim. Acta 368 (2021).

[86] W. Huang, Z. Bi, N. Zhao, Q. Sun, X. Guo, Chemical interface engineering of solid garnet batteries for long-life and high-rate performance, Chem. Eng. J. 424 (2021).

[87] E.J. Cheng, M. Shoji, T. Abe, K. Kanamura, Ionic liquid-containing cathodes empowering ceramic solid electrolytes, iScience 25 (2022) 103896.

[88] H. Huo, Y. Chen, R. Li, N. Zhao, J. Luo, J.G. Pereira da Silva, R. Mücke, P. Kaghazchi, X. Guo, X. Sun, Design of a mixed conductive garnet/Li interface for dendrite-free solid lithium metal batteries, Energy Environ. Sci. 13 (2020) 127–134.

[89] L. Liu, X. Qi, Q. Ma, X. Rong, Y.S. Hu, Z. Zhou, H. Li, X. Huang, L. Chen, Toothpaste-like electrode: a novel approach to optimize the interface for solid-state sodium-ion batteries with ultralong cycle life, ACS Appl. Mater. Interfaces 8 (2016) 32631–32636.

[90] E. Umeshbabu, B. Zheng, J. Zhu, H. Wang, Y. Li, Y. Yang, Stable cycling lithium-sulfur solid batteries with enhanced $Li/Li_{10}GeP_2S_{12}$ solid electrolyte interface stability, ACS Appl. Mater. Interfaces 11 (2019) 18436–18447.

[91] Y. Li, S. Halacoglu, V. Shreyas, W. Arnold, X. Guo, Q. Dou, J.B. Jasinski, B. Narayanan, H. Wang, Highly efficient interface stabilization for ambient-temperature quasi-solid-state sodium metal batteries, Chem. Eng. J. 434 (2022).

[92] K. Nie, Y. Hong, J. Qiu, Q. Li, X. Yu, H. Li, L. Chen, Interfaces between cathode and electrolyte in solid state lithium batteries: challenges and perspectives, Front. Chem. 6 (2018) 616.

[93] F. Sagane, T. Abe, Z. Ogumi, Electrochemical analysis of lithium-ion transfer reaction through the interface between ceramic electrolyte and ionic liquids, J. Electrochem. Soc. 159 (2012) A1766–A1769.

[94] T. Evans, D.M. Piper, H. Sun, T. Porcelli, S.C. Kim, S.S. Han, Y.S. Choi, C. Tian, D. Nordlund, M.M. Doeff, C. Ban, S.J. Cho, K.H. Oh, S.H. Lee, *In situ* engineering of the electrode-electrolyte interface for stabilized overlithiated cathodes, Adv. Mater. 29 (2017).

[95] H. Li, J. Pang, Y. Yin, W. Zhuang, H. Wang, C. Zhai, S. Lu, Application of a nonflammable electrolyte containing Pp13TFSI ionic liquid for lithium-ion batteries using the high capacity cathode material $Li[Li_{0.2}Mn_{0.54}Ni_{0.13}Co_{0.13}]O_2$, RSC Adv. 3 (2013) 13907.

[96] S. Sugata, N. Saito, A. Watanabe, K. Watanabe, J.-D. Kim, K. Kitagawa, Y. Suzuki, I. Honma, Quasi-solid-state lithium batteries using bulk-size transparent $Li_7La_3Zr_2O_{12}$ electrolytes, Solid State Ion. 319 (2018) 285–290.

[97] W. Feng, X. Dong, P. Li, Y. Wang, Y. Xia, Interfacial modification of Li/Garnet electrolyte by a lithiophilic and breathing interlayer, J. Power Sources 419 (2019) 91–98.

[98] A. Mauger, C.M. Julien, J.B. Goodenough, K. Zaghib, Tribute to Michel Armand: from rocking chair – Li-ion to solid-state lithium batteries, J. Electrochem. Soc. 167 (2020).

[99] J. Zhou, T. Qian, J. Liu, M. Wang, L. Zhang, C. Yan, High-safety all-solid-state lithium-metal battery with high-ionic-conductivity thermoresponsive solid polymer electrolyte, Nano Lett. 19 (2019) 3066–3073.

[100] T. Fuchs, B. Mogwitz, S.K. Otto, S. Passerini, F.H. Richter, J. Janek, Working principle of an ionic liquid interlayer during pressureless lithium stripping on $Li_{6.25}Al_{0.25}La_3Zr_2O_{12}$ (LLZO) garnet-type solid electrolyte, Batter Supercaps 4 (2021) 1145–1155.

[101] P. Hartmann, T. Leichtweiss, M.R. Busche, M. Schneider, M. Reich, J. Sann, P. Adelhelm, J. Janek, Degradation of NASICON-type materials in contact with lithium metal: formation of mixed conducting interphases (MCI) on solid electrolytes, J. Phys. Chem. C 117 (2013) 21064–21074.

[102] H. Chung, B. Kang, Mechanical and thermal failure induced by contact between a $Li_{1.5}Al_{0.5}Ge_{1.5}(PO_4)_3$ solid electrolyte and Li metal in an all solid-state Li cell, Chem. Mater. 29 (2017) 8611–8619.

[103] P. Schmitz, R. Jakelski, M. Pyschik, K. Jalkanen, S. Nowak, M. Winter, P. Bieker, Decomposition of imidazolium-based ionic liquids in contact with lithium metal, ChemSusChem 10 (2017) 876–883.

[104] P. Schmitz, M. Kolek, M. Pyschik, K. Jalkanen, S. Nowak, M. Winter, P. Bieker, Modified imidazolium-based ionic liquids with improved chemical stability against lithium metal, ChemistrySelect 2 (2017) 6052–6056.

[105] H. Yildirim, J.B. Haskins, C.W. Bauschlicher Jr., J.W. Lawson, Decomposition of ionic liquids at lithium interfaces. 1. Ab initio molecular dynamics simulations, J. Phys. Chem. C 121 (2017) 28214–28234.

[106] J. Tang, L. Wang, C. Tian, C. Chen, T. Huang, L. Zeng, A. Yu, Double-protected layers with solid-liquid hybrid electrolytes for long-cycle-life lithium batteries, ACS Appl. Mater. Interfaces 14 (2022) 4170–4178.

[107] H. Huo, Y. Chen, R. Li, N. Zhao, J. Luo, J.G.P. da Silva, R. Mücke, P. Kaghazchi, X. Guo, X. Sun, Design of a mixed conductive garnet/Li interface for dendrite-free solid lithium metal batteries, Energy Environ. Sci. 13 (2020) 127–134.

[108] Y. Zhong, Y. Xie, S. Hwang, Q. Wang, J.J. Cha, D. Su, H. Wang, A highly efficient all-solid-state lithium/electrolyte interface induced by an energetic reaction, Angew. Chem. Int. Ed. 59 (2020) 14003–14008.

[109] K. Shi, Z. Wan, L. Yang, Y. Zhang, Y. Huang, S. Su, H. Xia, K. Jiang, L. Shen, Y. Hu, *In situ* construction of an ultra-stable conductive composite interface for high-voltage all-solid-state lithium metal batteries, Angew. Chem. 132 (2020) 11882–11886.

[110] B. Zheng, J. Zhu, H. Wang, M. Feng, E. Umeshbabu, Y. Li, Q.-H. Wu, Y. Yang, Stabilizing $Li_{10}SnP_2S_{12}$/Li interface via an *in situ* formed solid electrolyte interphase layer, ACS Appl. Mater. Interfaces 10 (2018) 25473–25482.

[111] F. Wu, S. Fang, M. Kuenzel, T. Diemant, J.-K. Kim, D. Bresser, G.-T. Kim, S. Passerini, Bilayer solid electrolyte enabling quasi-solid-state lithium-metal batteries, J. Power Sources 557 (2023).

[112] Z. Chen, D. Stepien, F. Wu, M. Zarrabeitia, H.P. Liang, J.K. Kim, G.T. Kim, S. Passerini, Stabilizing the $Li_{1.3}Al_{0.3}Ti_{1.7}$ (PO_4) $_3$|Li interface for high efficiency and long lifespan quasi-solid-state lithium metal batteries, ChemSusChem 15 (2022), e202200038.

[113] Z. Chen, G.T. Kim, J.K. Kim, M. Zarrabeitia, M. Kuenzel, H.P. Liang, D. Geiger, U. Kaiser, S. Passerini, Highly stable quasi-solid-state lithium metal batteries: reinforced $Li_{1.3}Al_{0.3}Ti_{1.7}(PO_4)_3$/Li interface by a protection interlayer, Adv. Energy Mater. 11 (2021) 2101339.

[114] M.R. Busche, T. Drossel, T. Leichtweiss, D.A. Weber, M. Falk, M. Schneider, M. L. Reich, H. Sommer, P. Adelhelm, J. Janek, Dynamic formation of a solid-liquid electrolyte interphase and its consequences for hybrid-battery concepts, Nat. Chem. 8 (2016) 426–434.

[115] L. Han, M.L. Lehmann, J. Zhu, T. Liu, Z. Zhou, X. Tang, C.-T. Heish, A.P. Sokolov, P. Cao, X.C. Chen, T. Saito, Recent developments and challenges in hybrid solid electrolytes for lithium-ion batteries, Front. Energy Res. 8 (2020).

[116] M. Keller, A. Varzi, S. Passerini, Hybrid electrolytes for lithium metal batteries, J. Power Sources 392 (2018) 206–225.
[117] J.K. Kim, J. Scheers, T.J. Park, Y. Kim, Superior ion-conducting hybrid solid electrolyte for all-solid-state batteries, ChemSusChem 8 (2015) 636–641.
[118] H.W. Kim, P. Manikandan, Y.J. Lim, J.H. Kim, S.-c. Nam, Y. Kim, Hybrid solid electrolyte with the combination of $Li_7La_3Zr_2O_{12}$ ceramic and ionic liquid for high voltage pseudo-solid-state Li-ion batteries, J. Mater. Chem. A 4 (2016) 17025–17032.
[119] J. Hu, Z. Yao, K. Chen, C. Li, High-conductivity open framework fluorinated electrolyte bonded by solidified ionic liquid wires for solid-state Li metal batteries, Energy Storage Mater. 28 (2020) 37–46.
[120] Y. Yang, Q. Wu, D. Wang, C. Ma, Z. Chen, Q. Su, C. Zhu, C. Li, Ionic liquid enhanced composite solid electrolyte for high-temperature/long-life/dendrite-free lithium metal batteries, J. Membr. Sci. 612 (2020).
[121] Y. Zhai, W. Hou, M. Tao, Z. Wang, Z. Chen, Z. Zeng, X. Liang, P. Paoprasert, Y. Yang, N. Hu, S. Song, Enabling high-voltage "Superconcentrated Ionogel-in-Ceramic" hybrid electrolyte with ultrahigh ionic conductivity and single Li(+)-ion transference number, Adv. Mater. 34 (2022), e2205560.
[122] M. Liu, S. Zhang, E.R.H. van Eck, C. Wang, S. Ganapathy, M. Wagemaker, Improving Li-ion interfacial transport in hybrid solid electrolytes, Nat. Nanotechnol. 17 (2022) 959–967.
[123] R. Sampathkumar, M.G.K. Babu, E. Kurian, R.N. Ramesha, D. Bosubabu, K. Ramesha, Influence of lithium metal anode coated with a composite quasi-solid electrolyte on stabilizing the interface of all-solid-state battery, Ionics 28 (2022) 2649–2660.
[124] C. de la Torre-Gamarra, G.B. Appetecchi, U. Ulissi, A. Varzi, A. Varez, S. Passerini, $Na_3Si_2Y_{0.16}Zr_{1.84}PO_{12}$-ionic liquid hybrid electrolytes: An approach for realizing solid-state sodium-ion batteries? J. Power Sources 383 (2018) 157–163.
[125] A. Paolella, G. Bertoni, W. Zhu, D. Campanella, A. La Monaca, G. Girard, H. Demers, A.C. Gheorghe Nita, Z. Feng, A. Vijh, A. Guerfi, M. Trudeau, M. Armand, S.A. Krachkovskiy, Unveiling the cation exchange reaction between the NASICON $Li_{1.5}Al_{0.5}Ge_{1.5}(PO_4)_3$ solid electrolyte and the pyr13TFSI ionic liquid, J. Am. Chem. Soc. 144 (2022) 3442–3448.
[126] Z. Zhang, X. Wang, X. Li, J. Zhao, G. Liu, W. Yu, X. Dong, J. Wang, Review on composite solid electrolytes for solid-state lithium-ion batteries, Mater. Today Sustain. 21 (2023).
[127] F. Lv, Z. Wang, L. Shi, J. Zhu, K. Edström, J. Mindemark, S. Yuan, Challenges and development of composite solid-state electrolytes for high-performance lithium ion batteries, J. Power Sources 441 (2019).
[128] Z. Zou, Y. Li, Z. Lu, D. Wang, Y. Cui, B. Guo, Y. Li, X. Liang, J. Feng, H. Li, C. W. Nan, M. Armand, L. Chen, K. Xu, S. Shi, Mobile ions in composite solids, Chem. Rev. 120 (2020) 4169–4221.
[129] H. Huo, N. Zhao, J. Sun, F. Du, Y. Li, X. Guo, Composite electrolytes of polyethylene oxides/garnets interfacially wetted by ionic liquid for room-temperature solid-state lithium battery, J. Power Sources 372 (2017) 1–7.
[130] A. Heist, S.-H. Lee, Improved stability and rate capability of ionic liquid electrolyte with high concentration of LiFSI, J. Electrochem. Soc. 166 (2019) A1860–A1866.
[131] X. Gao, F. Wu, A. Mariani, S. Passerini, Concentrated ionic-liquid-based electrolytes for high-voltage lithium batteries with improved performance at room temperature, ChemSusChem 12 (2019) 4185–4193.
[132] F. Chen, P. Howlett, M. Forsyth, Na-ion solvation and high transference number in superconcentrated ionic liquid electrolytes: a theoretical approach, J. Phys. Chem. C 122 (2017) 105–114.
[133] Y. Zhao, L. Wang, Y. Zhou, Z. Liang, N. Tavajohi, B. Li, T. Li, Solid polymer electrolytes with high conductivity and transference number of Li ions for Li-based rechargeable batteries, Adv. Sci. 8 (2021), 2003675 (Weinh).
[134] Q. Zhou, J. Ma, S. Dong, X. Li, G. Cui, Intermolecular chemistry in solid polymer electrolytes for high-energy-density lithium batteries, Adv. Mater. 31 (2019), e1902029.
[135] A.D. Godwin, M. Kutz, Applied Plastics Engineering Handbook, Second Ed., William Andrew Publishing, 2017, pp. 533–553, https://doi.org/10.1016/B978-0-323-39040-8.00025-0.
[136] M. Kumar, S. Sekhon, Ionic conductance behaviour of plasticized polymer electrolytes containing different plasticizers, Ionics 8 (2002) 223–233.
[137] G. Hirankumar, N. Mehta, Effect of incorporation of different plasticizers on structural and ion transport properties of PVA-$LiClO_4$ based electrolytes, Heliyon 4 (2018), e00992.
[138] A.S.F.M. Asnawi, M.H. Hamsan, S.B. Aziz, M.F.Z. Kadir, J. Matmin, Y.M. Yusof, Impregnation of [Emim]Br ionic liquid as plasticizer in biopolymer electrolytes for EDLC application, Electrochim. Acta 375 (2021) 137923.
[139] I. Osada, H. de Vries, B. Scrosati, S. Passerini, Ionic-liquid-based polymer electrolytes for battery applications, Angew. Chem. 55 (2016) 500–513.
[140] Y. Lin, K. Liu, M. Wu, C. Zhao, T. Zhao, Enabling solid-state Li metal batteries by *In Situ* forming ionogel interlayers, ACS Appl. Energy Mater. 3 (2020) 5712–5721.
[141] L. Dong, X. Zeng, J. Fu, L. Chen, J. Zhou, S. Dai, L. Shi, Cross-linked ionic copolymer solid electrolytes with loose Coordination-assisted lithium transport for lithium batteries, Chem. Eng. J. 423 (2021).
[142] D. Cai, X. Wu, J. Xiang, M. Li, H. Su, X. Qi, X. Wang, X. Xia, C. Gu, J. Tu, Ionic-liquid-containing polymer interlayer modified PEO-based electrolyte for stable high-voltage solid-state lithium metal battery, Chem. Eng. J. 424 (2021).
[143] J. Li, Y. Cai, Y. Cui, H. Wu, H. Da, Y. Yang, H. Zhang, S. Zhang, Fabrication of asymmetric bilayer solid-state electrolyte with boosted ion transport enabled by charge-rich space charge layer for -20~70°C lithium metal battery, Nano Energy 95 (2022).
[144] J. Tan, X. Ao, A. Dai, Y. Yuan, H. Zhuo, H. Lu, L. Zhuang, Y. Ke, C. Su, X. Peng, B. Tian, J. Lu, Polycation ionic liquid tailored PEO-based solid polymer electrolytes for high temperature lithium metal batteries, Energy Storage Mater. 33 (2020) 173–180.
[145] X. Zhang, Q. Su, G. Du, B. Xu, S. Wang, Z. Chen, L. Wang, W. Huang, H. Pang, Stabilizing solid-state lithium metal batteries through *In Situ* generated janus-heterarchical LiF-rich SEI in ionic liquid confined 3D MOF/polymer membranes, Angew. Chem. (2023), e202304947, https://doi.org/10.1002/anie.202304947.
[146] I. Osada, H. deVries, B. Scrosati, S. Passerini, Ionic-liquid-based polymer electrolytes for battery applications, Angew. Chem. Int. Ed. 55 (2016) 500–513.
[147] Z. Liu, A. Borodin, F. Endres, Ionic liquid and polymer coated garnet solid electrolytes for high-energy solid-state lithium metal batteries, Energy Technol. 10 (2021).
[148] Y. Koizumi, D. Mori, S. Taminato, O. Yamamoto, Y. Takeda, N. Imanishi, Lithium-stable NASICON-type lithium-ion conducting solid electrolyte film coated with a polymer electrolyte, Solid State Ion. 337 (2019) 101–106.
[149] M. Watanabe, S.-i. Yamad, N. Ogata, Ionic conductivity of polymer electrolytes containing room temperature molten salts based on pyridinium halide and aluminium chloride, Electrochim. Acta 40 (1995) 2285–2288.
[150] M. Forsyth, L. Porcarelli, X. Wang, N. Goujon, D. Mecerreyes, Innovative electrolytes based on ionic liquids and polymers for next-generation solid-state batteries, Acc. Chem. Res. 52 (2019) 686–694.
[151] M.J. Park, I. Choi, J. Hong, O. Kim, Polymer electrolytes integrated with ionic liquids for future electrochemical devices, J. Appl. Polym. Sci. 129 (2013) 2363–2376.
[152] A.S. Shaplov, R. Marcilla, D. Mecerreyes, Recent advances in innovative polymer electrolytes based on poly(ionic liquid)s, Electrochim. Acta 175 (2015) 18–34.
[153] T. Chen, W. Kong, Z. Zhang, L. Wang, Y. Hu, G. Zhu, R. Chen, L. Ma, W. Yan, Y. Wang, J. Liu, Z. Jin, Ionic liquid-immobilized polymer gel electrolyte with self-healing capability, high ionic conductivity and heat resistance for dendrite-free lithium metal batteries, Nano Energy 54 (2018) 17–25.
[154] Y. Jiang, X. Yan, Z. Ma, P. Mei, W. Xiao, Q. You, Y. Zhang, Development of the PEO based solid polymer electrolytes for all-solid state lithium ion batteries, Polymers (Basel) 10 (2018).
[155] W. Qian, J. Texter, F. Yan, Frontiers in poly(ionic liquid)s: syntheses and applications, Chem. Soc. Rev. 46 (2017) 1124–1159.
[156] T.C. Mendes, N. Goujon, N. Malic, A. Postma, J. Chiefari, H. Zhu, P.C. Howlett, M. Forsyth, Polymerized ionic liquid block copolymer electrolytes for all-solid-state lithium-metal batteries, J. Electrochem. Soc. 167 (2020), 070525.
[157] X. Tian, Y. Yi, P. Yang, P. Liu, L. Qu, M. Li, Y.S. Hu, B. Yang, High-charge density polymerized ionic networks boosting high ionic conductivity as quasi-solid electrolytes for high-voltage vatteries, ACS Appl. Mater. Interfaces 11 (2019) 4001–4010.
[158] S.Y. Zhang, Q. Zhuang, M. Zhang, H. Wang, Z. Gao, J.-K. Sun, J. Yuan, Poly (ionic liquid) composites, Chem. Soc. Rev. 49 (2020) 1726–1755.
[159] M. Lei, S. Fan, Y. Yu, J. Hu, K. Chen, Y. Gu, C. Wu, Y. Zhang, C. Li, NASICON-based solid state Li-Fe-F conversion batteries enabled by multi-interface-compatible sericin protein buffer layer, Energy Storage Mater. 47 (2022) 551–560.